



**TRIBHUVAN UNIVERSITY
INSTITUTE OF ENGINEERING
PULCHOWK CAMPUS**

**A
FINAL YEAR PROJECT REPORT
ON**

**ANALYSIS OF THE IMPACT OF EV PENETRATION ON PROTECTION
COORDINATION**

(Submitted to the Department of Electrical Engineering as partial fulfillment of the requirements for the Bachelor in Electrical Engineering)

(EE755)

PROJECT SUPERVISORS

Assoc. Prof. Jeetendra Chaudhary

Asst. Prof. Akhileshwar Mishra

PROJECT MEMBERS


Prem Kumar Yadav, 75BEL031

Ram Pukar Yadav, 075BEL035

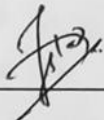
Sachidanand Sah, 075BEL038

Sashish Jha, 075BEL042


April 27, 2023


TRIBHUVAN UNIVERSITY
INSTITUTE OF ENGINEERING
PULCHOWK CAMPUS
DEPARTMENT OF ELECTRICAL ENGINEERING

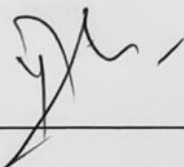
The undersigned certify that they have read, and recommended to the Institute of Engineering for acceptance, a project report entitled “**ANALYSIS OF THE IMPACT OF EV PENETRATION ON PROTECTION COORDINATION**” submitted by “*PREM KUMAR YADAV, RAMPUKAR YADAV, SACHIDANAND SAH, SASHISH JHA*” in partial fulfilment of the requirements for the Bachelor’s degree in Electrical Engineering.




Assoc. Prof. Jeetendra Chaudhary
Supervisor
Department of Electrical Engineering



Asst. Prof. Akhileshwar Mishra
Supervisor
Department of Electrical Engineering



Asst. Prof. Yubraj Adhikari
Head of the Department
Department of Electrical Engineering



Asst. Prof. Dr. Bishal Silwal
External Examiner
Department of Electrical and Electronics
Engineering
Kathmandu University

COPYRIGHTT©

The author has agreed that the Library, Department of Electrical Engineering, Pulchowk Campus, and Institute of Engineering may make this report freely available for inspection. Moreover, the author has agreed that permission for extensive copying of this project report for scholarly purposes may be granted by the supervisors who supervised the project work recorded herein or, in their absence, by the Head of the Department wherein the project report was done. It is understood that recognition will be given to the author of this report and to the Department of Electrical Engineering, Pulchowk Campus, Institute of Engineering in any use of the material of this project report. Copying or publication or the other use of this report for financial gain without the approval of the Department of Electrical Engineering, Pulchowk Campus, Institute of Engineering and the author's written permission is prohibited. Request for permission to copy or to make any other use of the material in this report in whole or in part should be addressed to:

The Head
Department of Electrical Engineering
Pulchowk Campus, Institute of Engineering
Lalitpur, Nepal

ACKNOWLEDGEMENT

First and foremost, we would like to express our sincere gratitude to our Supervisor **Assoc. Prof. Jeetendra Chaudhary** and **Asst. Prof. Akhileshwar Mishra** for his patience, motivation and continuous support in our project. We could not have imagined a better advisor and mentor.

We would like to express our deep respect to the Head of Electrical Engineering Department for his valuable and kind support.

Last but not least; we extend our special thanks to all the staff of the department and our friends and families for their cooperation. We are thankful to the authors of various research articles that we referred to during the course of the project.

Any sort of suggestions or criticism will be highly appreciated and acknowledged.

Prem Kumar Yadav

Rampukar Yadav

Sachidanand Sah

Sashish Jha

ABSTRACT

The global electric vehicle (EV) market has witnessed significant growth in recent years, driven by concerns over climate change, advances in battery technology, and supportive government policies. To address environmental pollution and the increasing energy consumption associated with conventional transportation systems, the adoption of EVs has emerged as a more sustainable alternative. However, the rapid increase in EV charging loads has raised significant operational challenges for power grids. This research project focuses on the impact of EV integration on relay and protection coordination in distribution systems.

Relay and protection coordination plays a crucial role in ensuring the safe and reliable operation of distribution systems by detecting abnormal conditions, such as faults or abnormal load conditions, and isolating the affected section to prevent further damage or outages. With the proliferation of EVs, the increased charging load introduces harmonic currents that can disrupt the operational parameters of the power grid. This study utilizes the IEEE standard 33 bus distribution system as a testbed to evaluate protection coordination using genetic optimization techniques.

By adding EV chargers at various nodes of the distribution system, the project assesses the time required for circuit breakers to trip in the event of a fault, evaluating the effectiveness of protection coordination techniques in the presence of EVs. The findings reveal that while the replacement of standard loads with EV chargers leads to a slight increase in the net RMS value of current and introduces harmonic currents, the sequence of relay operation remains unaltered. However, the relay operation time is affected, and in scenarios with bulk penetration of EV chargers, the increased harmonic current can cause overloading and other faults, resulting in relay trips.

To ensure the proper protection of the system, it is recommended to increase the pickup current for the relays. By adjusting the pickup current level, the relays will trip at higher current levels, mitigating false tripping caused by harmonic currents from EV chargers. The study emphasizes that meticulous design and planning are essential to maintain the reliability and protection of power distribution systems when integrating EV chargers.

This research contributes to the understanding of the challenges associated with protection coordination in distribution systems with the integration of EVs. The results underscore the importance of accounting for harmonic currents and adjusting relay settings to accommodate the increased demand associated with EV charging. Future work should focus on further optimizing protection coordination techniques to handle the growing penetration of EVs, ensuring the stability and reliability of power grids in the face of increasing environmental and energy demands.

TABLE OF CONTENTS

COPYRIGHTT©	iii
ACKNOWLEDGEMENT	iv
ABSTRACT.....	v
TABLE OF CONTENTS	vii
LIST OF FIGURES	x
LIST OF TABLES	xi
LIST OF ABBREVIATIONS	xii
CHAPTER ONE: INTRODUCTION.....	1
1.1 Background.....	1
1.2 Problem Statement.....	2
1.3 Objectives	2
1.4 Scope and Limitation.....	2
1.5 Project Report Overview	3
CHAPTER TWO: LITERATURE REVIEW	4
2.1 Distribution Network.....	4
2.2 Electric Vehicle	5
2.3 Distance Relay	6
2.4 Overcurrent Relay.....	6
2.5 Circuit Breaker.....	7
2.6 Genetic Algorithm.....	7
2.7 Protection Philosophy	9
2.7.1 Zone of protection:.....	10
2.7.2 Minimum fault current magnitude:.....	10
2.7.3 Relay pickup:	10
2.7.4 Relay operating time:.....	10

2.7.5 Coordinating time interval:	10
2.7.6 Relay:	11
2.8 Fault Types:.....	11
2.8.1 Transient fault:	11
2.8.2 Persistent fault:	12
2.8.3 Symmetrical fault:.....	12
2.8.4 Asymmetrical fault:.....	12
2.8.5 Bolted fault:	13
2.9 Overcurrent Protection for radial feeder	13
2.10 Overcurrent Protection for mesh feeder.....	13
2.11 Primary and Backup Protection	14
CHAPTER THREE: METHODOLOGY	16
3.1 Overview.....	16
3.2 Modeling of IEEE Standard 33 Bus distribution system.....	17
3.3 Load Flow and short-circuit analogies.....	18
3.4 Relay Characteristics	18
3.5 Protection Coordination using Genetic Algorithm (GA).....	20
3.5.1 Introduction of GA.....	20
3.5.2 Problem Definition	21
3.5.3 Methodology.....	23
3.6 Modeling of EV Charger and Analysis of EV charger	24
CHAPTER FOUR: RESULT AND DISCUSSION.....	26
4.1 Basic Introduction.....	26
4.2 Simulation of IEEE 33 Bus System.....	26
4.3 Protective device coordination.....	27
4.4 FFT Analysis.....	29

4.4.1 When lump loads are replaced with same ratings EV Charger load.....	31
4.4.2 When lump loads are replaced with rating of Standard EV Charger load.....	33
CHAPTER FIVE: CONCLUSION AND RECOMMENDATION	38
REFERENCES	40
APPENDIX.....	43
Appendix A: IEEE 33 Bus Distribution System.....	43
Appendix B: Modelling and Results.....	46
Appendix C: Genetic Algorithm Source Code	51

LIST OF FIGURES

Figure 2.1 Radial Distribution system	5
Figure 2. 2 Typical primary relay protection zones in a power system	9
Figure 2.3 Primary and Backup protection of Relay	14
Figure 3.1 Flowchart of Methodology	16
Figure 3.2 IEEE 33 bus model.....	17
Figure 3.3 Relay Characteristic Graph	20
Figure 3.4 A radial feeder both relays are non-directional	22
Figure 3.5 Flowchart of GA.....	24
Figure 3.6 Block diagram of EV charger [1]	25
Figure 4.1 GA scores and histograms	27
Figure 4.2 Voltage and current graph.....	29
Figure 4.3 FFT analysis of current of EV charger	31
Figure 4.4 Current plot when loads are replaced with the same ratings EV charger.....	31
Figure 4.5 Current plot when loads are replaced with Standard EV charger loads	34
Figure 4.6 IEE 33 Bus with EV charging stations and Sequence trip	37
Figure A.1 ETAP model of 33 bus distribution network	45
Figure B.1 EV charger model developed using MATLAB.....	46

LIST OF TABLES

Table 3.1 IEE 33 Bus Standard Bus.....	17
Table 3.2 Relay Equation Table	18
Table 4.1 Load Flow Report	26
Table 4. 2 Plug Setting and Time Multiplier Setting	28
Table 4. 3 Harmonics order present in EV charger.....	30
Table 4.4 Difference of currents when loads are replaced with same ratings EV charger ..	32
Table 4.5 Difference of Currents when loads are replaced with Standard EV charger	33
Table 4.6 Sequence of Operation of relay.....	35
Table 4.7 Sequence of Operation of relay with EV load	36
Table A.1 IEEE 33 Bus Distribution System Standard Data	43
Table B.1 Load flow report.....	46
Table B.2 Current distortions due to harmonics	49
Table B.3 Current distortions due to harmonics	50

LIST OF ABBREVIATIONS

AC	Alternating Current
THD	Total harmonic distortion
BEV	Battery Electric Vehicles
CB	Circuit Breaker
DC	Direct Current
EPRI	Electric Power Research Institute
EV	Electric Vehicle
ETAP	Electrical Transient and Analysis Program
GA	Genetic Algorithm
G2V	Grid-To-Vehicle
IEEE	Institute of Electrical and Electronics Engineers
IP	Integer Programming
IEC	International Electrotechnical Commission
LP	Linear Programming
MATLAB	Matrix Laboratory
NLP	Non-Linear Programming
PSM	Plug Setting Multiplier
PHEV	Plug-In-Hybrid Electric Vehicle
PFC	Power Factor Control
RMS	Root Mean Square
SAE	Society of Automotive Engineers
TMS	Time Multiplier Setting.
TCC	Time-Current Characteristics
V2G	Vehicle-To-Grid

CHAPTER ONE: INTRODUCTION

1.1 Background

In recent times, the electric vehicle (EV) market worldwide has been experiencing a fast-paced growth, mainly fueled by a surge in environmental awareness, improvements in battery technology, and government policies that support the adoption of EVs. In addition, many automotive manufacturers have been investing heavily in the development of EVs, and there are now a wide range of models available in the market, including battery electric vehicles (BEVs), plug-in-hybrid electric vehicle (PHEVs), and extended-range electric vehicle (EREVs). The electric vehicle (EV) market in Nepal is in its early stages of development. There have been some developments in the Nepalese EV market, with a small number of charging stations being established in major cities. However, the adoption of EVs in Nepal has been slow due to a number of factors, including a lack of charging infrastructure, high cost, and limited availability of models. It was found that EV disrupts protection coordination in the countries where EV penetration was done in large scale. so, we are going to study the impact of penetration of EV stations on the protection coordination of distribution systems.

A distribution system, also known as an electrical distribution system or power distribution system, is an essential component of the overall electrical power infrastructure. It is responsible for delivering electricity from the transmission system to end-users, such as residential, commercial, and industrial consumers. The distribution system plays a crucial role in ensuring the reliable and efficient supply of electricity to meet the diverse demands of users. In a radial distribution system, power flows in a unidirectional path from the source (substation) to the loads (consumers). It is the simplest and most common distribution system, often used in residential and small commercial areas. Distribution systems are vital for delivering electricity reliably and efficiently to end-users. With ongoing technological advancements and the evolving energy landscape, distribution systems are continuously adapting to meet the changing needs of consumers while striving for a sustainable and resilient energy future.

Protection relaying is a crucial component in the operation of power systems as it ensures the safety and reliability of the system. An important aspect of protection system design is relay coordination, which aims to achieve fast, selective, and reliable operation of relays to isolate faulted sections of the power system. During the planning stage of a power system, protective relaying is integrated with the overall system design. It involves the collaboration of various elements such as current transformers (CT), potential transformers (PT), protective relays, time delay relays, trip circuits, and circuit breakers. The coordination of these components enables the detection of abnormal conditions in specific parts of the power system, triggering alarms or isolating the affected section from the healthy portion of the system. Effective relay coordination also facilitates the ability to island generators and loads together, enhancing local reliability [1].

1.2 Problem Statement

The presence of a large number of EV charging stations results in the generation of harmonics, which can cause problems for the relay and its settings. As the number of charging stations increases, there is an increase in load and different types of harmonics, which may cause the relay to trip falsely or alter its operation time.

1.3 Objectives

□ To determine the effect of EV penetration on relay coordination in distribution system.

1.4 Scope and Limitation

The impact of electric vehicle (EV) penetration on protection coordination is a crucial area of study for the power system industry. Analyzing fault current levels, coordination of protection devices, voltage profile, and load demand with varying levels of EV penetration can provide valuable insights into the required protection coordination measures.

It is important to carefully study and analyze the impact of EV penetration on protection coordination to ensure that the power system remains stable and reliable. By gaining a thorough understanding of the potential impact, necessary modifications or upgrades to the protection coordination scheme can be identified. This will enable the power system to accommodate the integration of EVs effectively and efficiently, while maintaining stability and reliability.

As part of our study, we have focused solely on the radial distribution network. It is important to note that our results and outputs may not be equally applicable for other configurations of the distribution system, such as the meshed or ring distribution networks. The differences in the configuration and topology of these networks can impact the performance and behavior of the distribution system, and therefore, the results obtained in our study may not be directly transferable. This limitation should be taken into consideration when interpreting the results and conclusions of our study, and further research may be required to explore the impact of EV penetration on protection coordination in other distribution system configurations.

1.5 Project Report Overview

This project consists of the following chapters:

- This project constitutes five chapters including the current chapter. This chapter explains the importance of analysis of EV penetration on distribution networks. Also, it covers the statement of the problem, objectives of this project, scopes and limitations.
- Chapter two of this report presents a comprehensive literature review that encompasses theoretical articles, publications from IEEE conferences or transactions, and books from major publications. This review aims to collate existing information and prior findings related to the research topic
- Chapter three explains the methodology of work for modeling of IEEE standard 33 bus radial distribution system and coordination of relays.
- Chapter four presents the simulation results and discussions under various cases considered.
- Chapter five concludes the results and presents the further work to do.

CHAPTER TWO: LITERATURE REVIEW

2.1 Distribution Network

The distribution network plays a crucial role in power systems by directly connecting to the load center. The integration of renewable and distributed energy sources at the distribution level poses a major concern for power system engineers. As a result, power companies and engineers are continuously researching and developing improved techniques to enhance power quality and stability in distribution networks [3].

Establishing a reliable and stable distribution network is vital for efficient power delivery to the load center. A well-planned electrical power distribution system can improve power provision to individual customer premises. However, distribution networks are also vulnerable to natural disasters, such as earthquakes and cyclones. Since each system is designed with specific resilience criteria, any damage sustained can have a significant impact on power network restoration. The duration of restoration depends on factors such as the network's design, control, and management.

Typically, a distribution network comprises substations, primary feeders, transformers, distributors, and service mains. The efficient operation of these components is critical to ensure the reliable delivery of power to customers. Therefore, it is essential to implement appropriate strategies to safeguard the distribution network against potential threats, both natural and human-made, to maintain a stable and dependable power supply.[3].

Radial networks as shown in Figure 2.1, are the most common topology for power distribution grids. They have a tree-shaped structure without any closed loops, which makes it easy to deliver power from one bus to another without having to trace back to the source. However, if there's a line disconnection, all downstream lines lose power. Mesh networks, on the other hand, have additional redundant lines that act as backups to redirect power if the mainline fails. These networks are efficient for short-distance transmission and are great for incorporating renewable energy resources. The mesh structure can be upgraded from a radial network, and it's possible to efficiently utilize interface converters to connect

renewable energy resources. Overall, both radial and mesh network structures have their benefits, and choosing the appropriate one depends on various factors such as reliability, cost, and efficiency.[3].

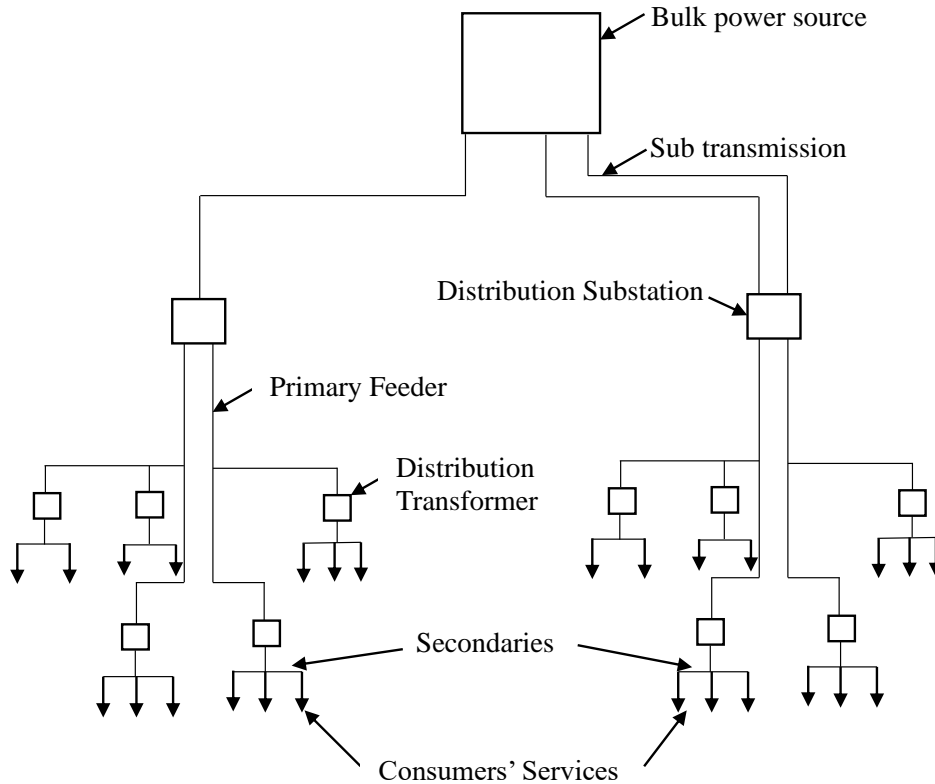


Figure 2.1 Radial Distribution system

2.2 Electric Vehicle

Electric Vehicles (EVs) are gaining popularity and are expected to have a significant role in future power systems. However, since EV chargers are a relatively new type of load, it is essential to investigate their impact on the dynamic behaviors of power systems. EV chargers are typically connected to the grid through power electronics, which may exhibit different dynamic behaviors compared to traditional loads. Therefore, it is crucial to carefully consider the dynamic responses of EVs and the modeling approaches used to represent their power electronic interfaces when analyzing stability and setting relays in power systems.

The behavior of EVs relies on the charging patterns of users and can become a substantial part of the electric load, particularly in specific locations and at certain times of the day.

Charging standards and power levels available for EV chargers vary, including AC level-1, AC level-2, and DC fast charging (level-3), as categorized by the Electric Power Research Institute (EPRI) and Society of Automotive Engineers (SAE). For example, AC level-2 chargers typically have a power output of 7.4 kW, while DC fast charging (level-3) provides 50 kW, and high-speed chargers like Tesla superchargers offer 350 kW or CHAdeMO 2.0 at 400 kW [1].

Detailed modeling approaches have been developed to accurately represent the dynamic behaviors of EV chargers, such as grid-to-vehicle (G2V), vehicle-to-grid (V2G), and residential charging. These approaches contribute to understanding the impact of EV chargers on the dynamic behavior of power systems and enhance stability analysis [1].

2.3 Distance Relay

Distance relays are protective devices employed to compare voltages and currents, creating impedance-plane and directional characteristics. Traditional electromechanical relays achieve this by generating torques, while static-analog implementations typically utilize coincidence-timing techniques. However, numerical techniques represent the latest approach for implementing distance and directional relay elements. These relays employ torque-like products and other methods to achieve their desired operating characteristics [2].

Phase angle comparators assess the angle between different combinations of voltage and current to generate directional, reactance, mho, and other characteristics. The most commonly utilized technologies for comparing phasors in relays include induction cylinders, coincidence timers, and digital multiplication. By analyzing the phase angle between the measured voltage and current, relays can identify faults within the power system and initiate protective actions to prevent equipment damage or harm to individuals [2].

2.4 Overcurrent Relay

An overcurrent relay is a crucial electrical protection device utilized to detect and isolate overcurrent conditions in power systems. It operates by comparing the current flowing through a circuit with a predetermined threshold level and trips the circuit breaker when the

current exceeds this threshold. Overcurrent relays can be time or instantaneous and can be either electromechanical, static, or microprocessor-based [17].

The coordination of overcurrent relays is crucial for the efficient protection of power systems. This coordination ensures that the relays closest to the fault trip first, avoiding unnecessary tripping of other relays and circuit breakers. It also helps to minimize the disruption of power supply and reduce the likelihood of equipment damage or personnel injury. With proper coordination, overcurrent relays can help maintain the stability and reliability of power systems, which is essential for ensuring the uninterrupted supply of electricity.

2.5 Circuit Breaker

A circuit breaker is an electrical switch designed to protect an electrical circuit from damage caused by excessive current, overload, or short circuit [18]. Its primary function is to interrupt the flow of current once protective relays detect a fault. Within a circuit breaker, there are two crucial contacts:

- Fixed contacts
- Moving contacts

During normal operation when the circuit is closed, these contacts make contact with each other and allow current to pass through. In a closed-circuit breaker, the contacts that carry the current are referred to as electrodes, which are held together by the pressure of a spring.

The circuit breaker's operation involves either opening or closing its arms to control the flow of electricity and perform maintenance tasks. Opening the circuit breaker is achieved by applying pressure to a trigger mechanism. When a faulty current is detected in any part of the system, the trip coil of the circuit breaker is energized, causing the contacts to move apart and thereby opening the circuit.

2.6 Genetic Algorithm

A genetic algorithm is a problem-solving method that is inspired by the process of natural selection in biological organisms. It is a type of optimization algorithm that is used to find the best solution to a problem in a large search space. The algorithm is derived from the

principles of genetics, which involve the idea of survival of the fittest. In a genetic algorithm, a population of potential solutions to a problem is generated, and then those solutions are evaluated to determine how well they solve the problem. The solutions that perform better are selected for reproduction, and their genetic material is combined to create new solutions. This process of selection, reproduction, and mutation continues until a satisfactory solution is found.

The genetic algorithm operates on a population of chromosomes, which represent potential solutions to the problem at hand. Each chromosome is a sequence of genes that encodes a possible solution. The genes are typically represented as binary digits, but they can also take other forms.

The genetic algorithm has several steps. First, an initial population of chromosomes is created randomly. Then, each chromosome is evaluated to determine its fitness score, which is a measure of how well it solves the problem. The chromosomes that have higher fitness scores are more likely to be selected for reproduction.

The next step is reproduction, where pairs of chromosomes are selected to create new offspring. This is done using crossover, which involves combining the genes of two parent chromosomes to create a new child chromosome. The mutation is also introduced, which randomly changes some genes in the offspring chromosome to increase diversity in the population.

The offspring chromosomes are then evaluated for fitness, and the process of selection, reproduction, and mutation continues for several generations until a satisfactory solution is found. The algorithm can be tuned by adjusting parameters such as the population size, the mutation rate, and the selection criteria.

The genetic algorithm is widely used in various fields, including engineering, computer science, economics, and biology. It is particularly useful for solving complex optimization problems where traditional methods are impractical or inefficient.

2.7 Protection Philosophy

Protective equipment plays a vital role in power systems as both primary and backup protection mechanisms. The primary protection acts as the initial defense line against faults and abnormal operating conditions. Its purpose is to promptly respond and minimize the impact on the power system, unlike the backup protection. Backup protection comes into action when the primary protection fails to clear the abnormal condition. These devices are set to activate after a specific time interval following the operation of the primary device. As a result, backup devices need to withstand fault conditions for a longer duration compared to the primary protective device.

When the backup device operates, it not only isolates the faulty or overloaded circuit but also additional circuits. This disconnection of a larger portion of the power system with backup protection is crucial in preventing further damage and ensuring system stability. Figure 2.2 provides a typical diagram illustrating different zones of protection. Zone including relay 5 is the primary protection zone. The zone bounded by relay 3 and relay 1 acts as secondary protection for zone including relay 5.

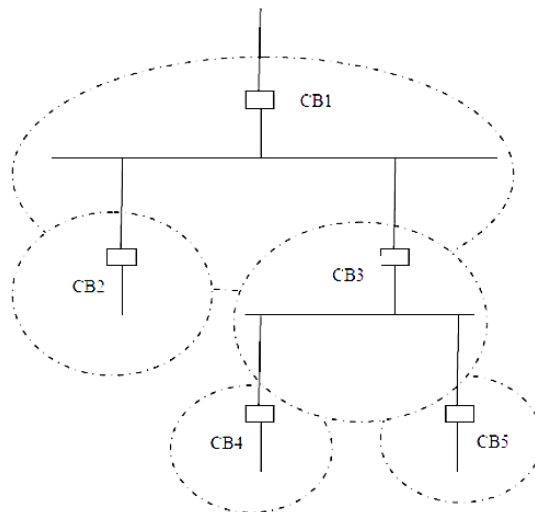


Figure 2. 2 Typical primary relay protection zones in a power system

When performing protection studies, the following terms are often used to make the language simpler and easier to understand:

2.7.1 Zone of protection:

The zone of protection for a relay refers to the specific area or distance that the relay can efficiently protect. This zone represents the sections of the power system where the relay will activate in response to a fault occurrence. The location of the fault within the primary or secondary zone will determine whether the relay serves as the primary protection or backup protection. Additionally, in some cases, there may be a tertiary zone designated for load encroachment. The precise definition and scope of the protection zone depend on the specific power system and the type of relay employed. Properly defined protection zones can help ensure that the relay functions effectively in detecting and isolating faults, thereby safeguarding the power system against further damage or failure [19].

2.7.2 Minimum fault current magnitude:

It refers to the lowest magnitude of fault current that the relay detects for any type of fault.

2.7.3 Relay pickup:

The pickup current setting is the minimum level of electrical current required to activate a protective relay. It represents the threshold at which the relay will begin to operate in response to a fault or abnormal condition in the power system. The PU setting is typically associated with a specific current magnitude that the relay will respond to, and it is critical for ensuring that the relay can detect and isolate faults effectively. Without an appropriate PU setting, a protective relay may fail to operate when needed, resulting in potential damage to the power system or even posing a risk to personnel.

2.7.4 Relay operating time:

It is the minimum time taken by the relay to operate.

2.7.5 Coordinating time interval:

The coordinating time interval, also known as the time difference between the operation of primary and secondary relays, is an important aspect of protective devices. This interval refers to the duration between the activation of the primary protection device and the subsequent activation of the secondary or backup protection device. The purpose of the

coordinating time interval is to allow the primary protection sufficient time to clear faults and abnormal conditions effectively. By introducing a delay, the secondary relay ensures that it only operates if the primary relay fails to clear the fault within the specified timeframe. This time delay is crucial in preventing unnecessary tripping of the system during transient or temporary faults. It provides a safeguard against false triggering and allows the primary protection to respond swiftly to faults while minimizing disruptions to the power system.

Coordinating the time interval between primary and secondary relays is a key consideration for maintaining the stability and reliability of the power system. It allows for an optimized coordination of protective devices, ensuring that faults are addressed promptly while providing an additional layer of protection if the primary protection fails to operate as intended.

2.7.6 Relay:

This component, whether electromechanical or digitally controlled, is responsible for operating the recloser, breaker, or switches.

2.8 Fault Types:

A fault in a power system refers to any condition that can cause abnormal current to flow in an undesired path or disrupts current flow in a desired path. This can include short or low-impedance circuits, power swings, over voltages, open circuits, elevated temperatures, and operation outside of nominal frequency. Faults can be caused by insulation failure, broken conductors, or external factors such as bird interference, kite string, or tree limbs. Depending on the nature of the fault, there are various types of faults that can occur in transmission lines.

2.8.1 Transient fault:

It is a type of fault that only occurs temporarily and can be rectified by disconnecting and restoring the power supply or by waiting for a short time until the insulation properties of the affected device are restored. Transient faults are common in overhead power lines and can occur due to various reasons such as lightning strikes, short-term overvoltage, or temporary line contact with trees or other objects. Unlike permanent faults, transient faults

do not cause permanent damage to the system and can be corrected without major repair or replacement of equipment [19].

2.8.2 Persistent fault:

A persistent fault is a type of fault that remains even when the power is disconnected. These types of faults are typically observed in underground power cables, and they are often caused by mechanical damage to the cable. In some cases, persistent faults can also be transient, which means they may only last for a short period and are caused by lightning. Persistent faults are problematic as they can cause a prolonged interruption in power supply until the fault is located and repaired.

2.8.3 Symmetrical fault:

A symmetric or balanced fault occurs when each of the three phases of a power system is affected equally, resulting in equal currents flowing through each phase. Such faults are relatively rare and typically account for only 5% of transmission line faults. On the other hand, an asymmetrical fault occurs when three phases of a power system are not affected equally, resulting in the flow of unbalanced current through each phase.

2.8.4 Asymmetrical fault:

An asymmetrical fault does not affect each of the three-phase equally. They are of three types as follows:

2.8.4.1 Line-to-line:

When two power transmission lines come into physical contact or the air surrounding them becomes ionized, it results in a fault known as a line-to-line fault. This fault can also occur when an insulator breaks. Asymmetric line-to-line faults, where the impact on the three phases is not equal, account for around 5% to 10% of transmission line faults.

2.8.4.2 Line-to-ground:

An asymmetric line-to-ground fault is a type of fault in which one of the power lines comes in contact with the ground, resulting in a short circuit. This kind of fault is frequently caused

by external factors such as lightning or storm damage. In transmission line faults, asymmetric line-to-ground faults account for approximately 65% - 70% of all faults.

2.8.4.3 Double line-to-ground:

An asymmetric double line-to-ground fault occurs when two power lines come into touch with the ground and each other, often caused by severe weather conditions such as storms. It accounts for approximately 15% to 20% of faults in transmission lines.

2.8.5 Bolted fault:

A "bolted fault" refers to a hypothetical situation where a fault in an electrical system has zero impedance, leading to the highest possible short-circuit current. In this scenario, it is assumed that all the conductors are directly linked to the ground, as if connected by a metallic conductor.

2.9 Overcurrent Protection for radial feeder

In radial feeder the current flowing is unidirectional. Protection in such a system is achieved by measuring the fault current (I_f). If the fault current is greater than the pick-up current, the relay will give trip signal and if fault current is less than the pickup current, the relay will not operate. i.e.

$I_f > I_p$ Relay Trip ON, $I_f < I_p$ Relay Trip OFF (BLOCK)

2.10 Overcurrent Protection for mesh feeder

In a mesh system, the current can flow in both directions, making it more challenging to identify the fault location and isolate it. This is why directional overcurrent relays are used as protective devices. These relays are designed to not only detect the magnitude of the current but also its direction.

Directional overcurrent relays operate based on the principle that current flows in opposite directions in different parts of the power system. By analyzing the current flow direction, the relay can identify the location of the fault and isolate it from the rest of the system.

2.11 Primary and Backup Protection

In power systems, it is crucial to have a reliable protection system in case of faults. However, there are instances when the primary protection system may fail, and a backup protection system becomes necessary. The backup protection system provides an additional line of defense and must be independent of the primary protection system. It is also preferable to have the backup protection system installed at a different location than the primary protection system to avoid any common failure modes.

The backup protection system should only trip the circuit breaker after the primary protection system has operated, ensuring that the fault is isolated correctly. The operating time of the backup protection system should be equal to the operating time of the primary protection system plus the operating time of the primary circuit breaker. The radial power system in Figure 2.3 illustrates the primary and backup protection systems.

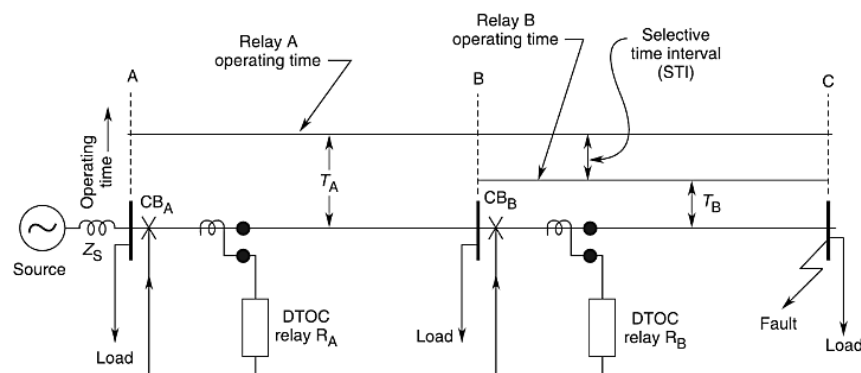


Figure 2.3 Primary and Backup protection of Relay

As per Figure 2.3, if there is a problem in one of the parts that deliver electricity (known as feeder elements), several or all relays located closer to the power source (between the problem and the supplying system) will activate and begin a countdown. However, only the relay closest to the problem is supposed to switch off and stop the flow of electricity. This relay has the shortest delay before it activates. Once it trips, the rest of the relays located upstream will reset and no more switches will be activated. The relays positioned downstream from the problem will not activate because there is no faulty current flowing in that area. The section of the electrical network downstream from the problem will be disconnected by the relay that operates. On the other hand, the part of the network upstream from the problem will continue to function normally once the fault is resolved.

If the designated relay or its associated breaker fails to function and clear the fault, the next relay located closer to the power source will step in as a backup protection measure. This upstream relay will activate and attempt to clear the fault. If it also fails to operate, the subsequent relay upstream will take action, and so on. In this scenario, more elements within the network will be tripped or switched off. Despite considering both the fault and potential equipment malfunction, this course of action is still considered the best option or optimal response.

CHAPTER THREE: METHODOLOGY

3.1 Work Overview

The flowchart presented in Figure 3.1 illustrates the fundamental approach adopted for our work. Our project was executed following the outlined methodology depicted in the flowchart.

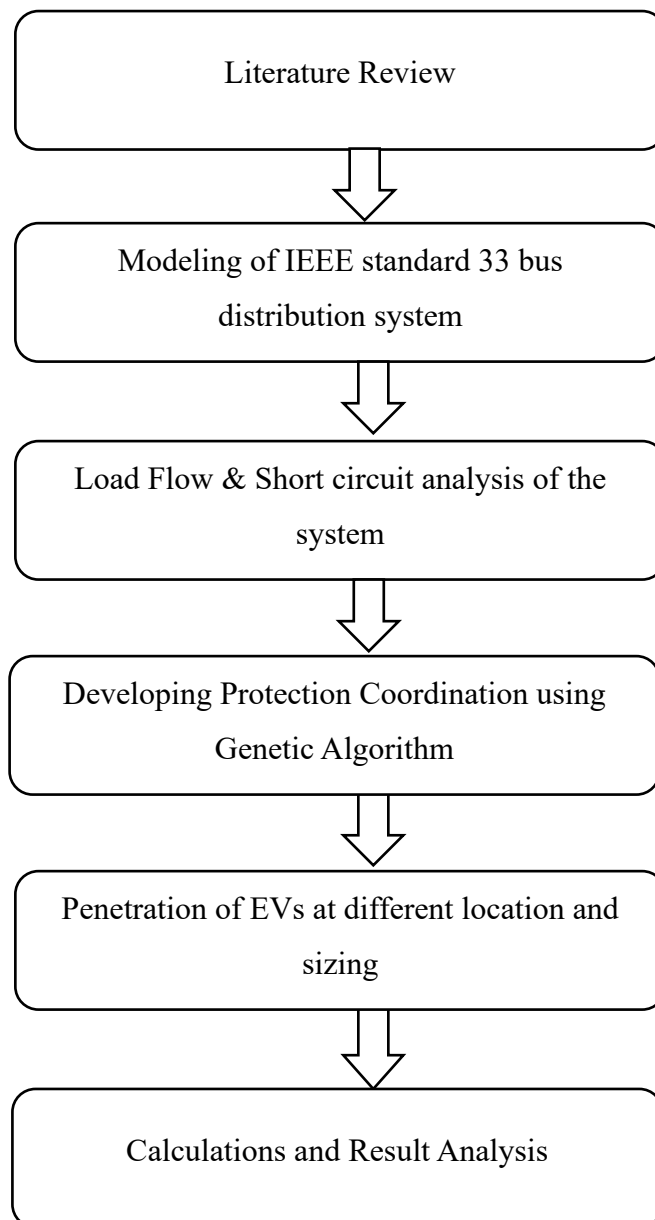


Figure 3.1 Flowchart of Methodology

Modeling of IEEE Standard 33 bus distribution system

The data for the IEEE 33 Bus standard system is obtained from the standard research document. This system is created in software like ETAP and MATLAB for simulation purposes, using the data from the document. To verify the accuracy of the simulation, the developed system is evaluated by the IEEE Distribution System standard result. Table 3.1 provides information about the impedance of the IEEE 33 Bus system. All 33 bus system parameters are shown in Table A.1 In simpler terms, the IEEE 33 Bus system can be modeled and analyzed using computer software, and its accuracy can be verified by research papers. Figure 3.2 shows the model of the standard IEE 33 Bus System. The ETAP model of the 33 bus distribution system is shown in Figure A.1.

Table 3.1 IEE 33 Bus Standard Bus

Branch Name	Path of Bus	Load Name	Length (km)	Real Load(Kw)	Reactive Load(Kvar)	Resistance (Ohm/km)	Reactance (Ohm/km)
Branch1	1-2	L2	1	100	60	0.0922	0.0470
Branch2	2-3	L3	1	90	40	0.493	0.251
Branch3	3-4	L4	1	120	80	0.366	0.186
Branch4	4-5	L5	1	60	30	0.3811	0.1941
Branch5	5-6	L6	1	60	20	0.819	0.707

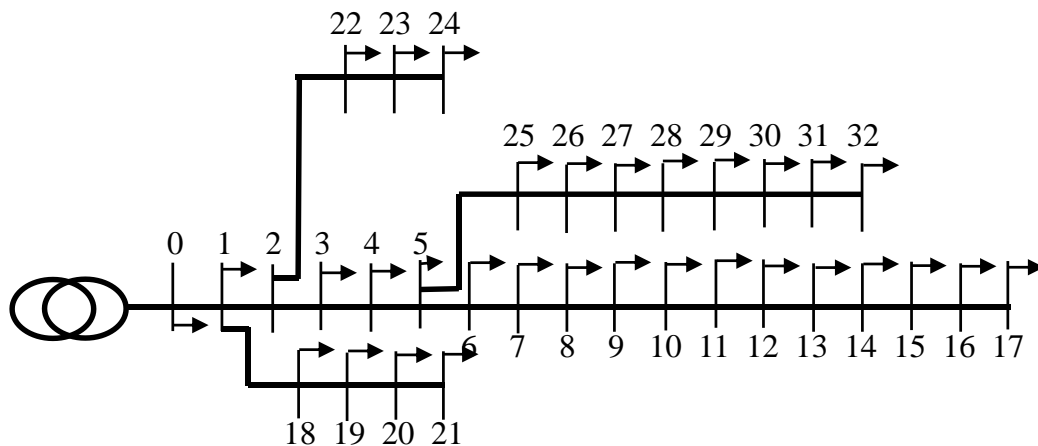


Figure 3.2 IEEE 33 bus model

3.2 Load Flow and short-circuit analogies

The ETAP software was utilized to perform load flow analysis on the aforementioned bus system. Following this, a short-circuit analysis was carried out on the system, where short-circuit conditions were created at various branches and buses to observe the performance of the system. By examining the load flow and short-circuit analysis results, the actual behavior of the radial distributed bus system was obtained. This information proved to be valuable in the development of an effective protection system for the network. Therefore, the load flow and short-circuit analysis played a crucial role in understanding the behavior of the bus system and protective measures to prevent damage.

$$\text{fault MVA} = \frac{\text{base MVA}}{Z_{pu}} \dots\dots\dots \text{Equation 3.1}$$

$$\text{fault KA} = \frac{\text{fault MVA}}{3 \times V_{LN}} \dots\dots\dots \text{Equation 3.2}$$

3.3 Relay Characteristics

The load flow study and short-circuit analysis provide an understanding of the overall behavior of the radial distribution system that has been developed. This information is essential in creating an effective protection system for the distribution network. Various protection systems, such as circuit breakers, fuses, re-closers, and relays, are employed to improve the coordination of protection in the simulated model. Overcurrent relays are used to protect the feeders, with an inverse time overcurrent protection being the preferred choice. The inverse time overcurrent protection works by having an operating time that is inversely proportional to the magnitude of the fault current. Different time-current characteristic curves are used, such as those defined by the IEC 60255 standard curves, as shown in Table 3.2. Overall, the load flow study and short-circuit analysis help create an appropriate protection system for the radial distribution system, which is critical in preventing damages and ensuring the system's proper functioning.

Table 3.2 Relay Equation Table

Relay Characteristics	Equations (IEC 60255)
Standard Inverse (SI)	$t = TMS * \frac{0.14}{I_r^{0.02-1}}$
Very Inverse (VI)	$t = TMS * \frac{13.5}{I_r - 1}$

Extremely Inverse (EI)	$t = \text{TMS} * \frac{80}{I_r^2 - 1}$
Long time stand by earth fault	$t = \text{TMS} * \frac{120}{I_r - 1}$

Where: $I_r = I/I_s$, Measured current, I_s = Relay setting current, TMS= Time Multiplier Setting.

The relays and reclosers in this study are equipped with a standard inverse characteristic curve. To ensure that the inverse time overcurrent relay operates effectively, the pickup current is set to 1.05 to 1.20 times the primary currents of the current transformer. The selection of primary currents is based on the maximum load currents that are expected. Additionally, the IEC normal inverse characteristic curve has a time multiplier setting of 0.2. To calculate the plug setting multiplier (PSM), the fault current is obtained from the short-circuit analysis. By utilizing this methodology, the appropriate settings for the protection systems can be established, which ensures that the system is protected against faults and operates optimally. Figure 3.3 shows the Time characteristics curve of a general OCR.

$$\text{PSM} = \frac{\text{Fault Current}(I_f)}{\text{Pickup Current}(I_s)} \dots\dots\dots \text{Equation 3.3}$$

The minimum time delay setting for the instantaneous element is 60 milliseconds for the high-voltage (HT) side and 40 milliseconds for the low-voltage side. To determine the time setting multiplier (TSM) for the standard inverse characteristic curve, you can calculate it using equation 3.3.

$$\text{TMS} = \frac{t * (\text{PMS})^{0.02} - 1}{0.14} \dots\dots\dots \text{Equation 3.4}$$

Where t is the time delay required.

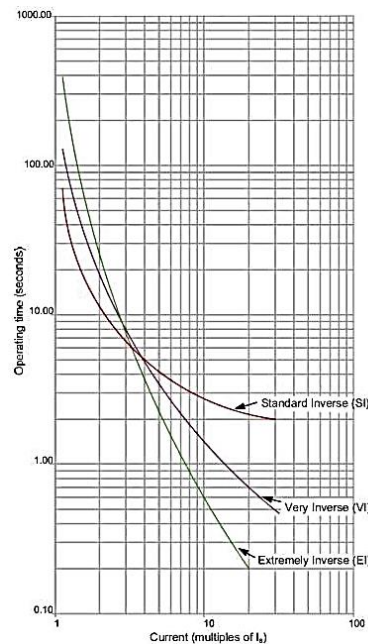


Figure 3.3 Relay Characteristic Graph

The goal of protection coordination in power systems is to ensure selectivity, which means that only the faulted component is switched off while the rest of the power system remains in operation. This minimizes disruptions in the power supply and helps maintain stability. Effective coordination ensures that protective devices neither malfunction nor duplicate their operation. To achieve selectivity in isolating a fault, protective devices are arranged in a series and time-coordinated. This means that the device closest to the short circuit or overload opens first to isolate the faulty section.

3.4 Protection Coordination using Genetic Algorithm (GA)

3.4.1 Introduction of GA

Power systems are made up of a multitude of equipment and protection relays to safeguard the system. Proper coordination of these relays is crucial to prevent mal-operation and ensure efficient protection. Coordination involves selecting time multiplier settings (TMS) and plug setting multipliers (PSM) that meet all constraints and operate within the shortest possible time. In systems where fault and load currents can flow in either direction due to sources at both ends of the line, directional overcurrent relays (OC) are used to avoid coordination with relays behind them. This coordination problem can be defined as a constrained optimization problem and can be solved using techniques such as GA. Coordinating relays in a power

system involves solving an optimization problem with numerous constraints, resulting in many local optimal solutions. Traditional methods like LP, NLP, and IP start the optimization from the first point, leading to a heavily dependent final solution. The use of optimization techniques can eliminate the need for finding minimum break points. In this context, a linear-programming approach is often used to minimize relay operating time based on coordination constraints, relay characteristics, and relay setting limits. However, a more effective approach is to use the GA algorithm to search for solutions from a population of primary points, which reduces the likelihood of being trapped in local optimal points. Nonetheless, GA algorithms can be time-consuming for large-scale problems with many constraints, making it necessary to find the optimal solution in the shortest possible time.

3.4.2 Problem Definition

The coordination problem associated with directional overcurrent (OC) relays in interconnected power systems can be formulated as an optimization task. The objective is to minimize the total operating times of the relays within the system for faults occurring in close proximity to the source[21].

$$\min z = \sum_{i=1}^n t_{i,i} \qquad \min z = \sum_{i=1}^n t_{i,i} \qquad \dots\dots\dots \text{Equation 3.5}$$

Subjected to the following inequality constraints

$$t_{j,i} - t_{i,i} \geq \Delta t \qquad \dots\dots\dots \text{Equation 3.5}$$

$$t_{i,i,\min} \leq t_{i,i} \leq t_{i,i,\max} \qquad \dots\dots\dots \text{Equation 3.5}$$

$$(t_{op})_i = \frac{\lambda(TMS)_i}{(PSM)_i^\gamma - 1} \qquad \dots\dots\dots \text{Equation 3.5}$$

For normal Inverse definite minimum time (IDMT) relay γ is 0.02 and λ is 0.14., equation (3.5) becomes[21]

$$t_{op} = a_i (TMS)_i \qquad \dots\dots\dots \text{Equation 3.5}$$

$$a_i = \frac{\lambda}{(PSM)_i^\gamma - 1} \qquad \dots\dots\dots \text{Equation 3.5}$$

and $PSM = I/I_s$

Making substitution from equation (3.5) in equation (3.5), the objective function becomes

$$\min z = \sum_{i=1}^n a_i (TMS)_i \quad \text{..... Equation 3.5}$$

This is a non-linear optimization problem.

Where;

$t_{i,i}$ is the operating time of the primary relay at i, for near end fault.

$t_{j,i}$ is the operating time for the backup relay, for the same near end fault.

Δt is the coordination time interval (CTI).

$t_{i,i,\min}$ is the minimum operating time of relay at i for near end fault (fault at i).

$t_{i,i,\max}$ is the maximum operating time of relay at i for near end fault (fault at i).

t_{op} is the relay operating time.

I is the input current.

I_s is the setting current.

TMS is time multiplier setting, and

PSM is plug setting multiplier.

Coordination of over current relay can be easily understood by this simple radial system and the same concept can be applied for larger system also using algorithm:

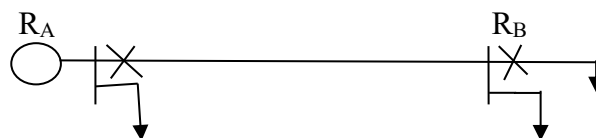


Figure 3.4 A radial feeder both relays are non-directional[21]

Maximum fault current beyond bus A: 4 kA

Maximum fault current beyond bus B: 3 kA

Plug setting of both relays: 100%

CT ratio of relay A (RA): 300:1

CT ratio of relay B (RB): 100:1

Minimum operating time of each relay: 0.25 seconds

CTI: 0.57 seconds

For this system Coordination problem is

$$\text{Min } Z = 2.63X_1 + 2 X_2$$

Where X_1 and X_2 is TMS of relay R_A and R_B

Subject to:

$$2.97X_1 - 2X_2 \geq 0.57$$

$$2.63 X_1 \geq 0.2$$

$$2X_2 \geq 0.2$$

Using GA

$$(\text{TMS})_A = 0.682 \text{ sec and } (\text{TMS})_B = 0.2 \text{ sec}$$

3.4.3 Methodology

For this study, the IEEE 33-bus distribution network was utilized and modeled with ETAP software, where the electrical parameters were adjusted to the desired values. Load flow analysis and short circuit analysis were conducted to determine the expected load current (IL), minimum fault current (IF, MIN), and maximum fault current (IF, MAX) for all network elements, which would be utilized as inputs during the relay setting process using GA. The optimization flowchart is depicted in the figure 3.5. The methodology employed in this algorithm begins by initializing the process and defining a fitness function to evaluate potential solutions. Input regarding the number of variables and stopping criteria is provided, and specific parameters for the Genetic Algorithm (GA) are established. An initial population is generated, and the fitness of each chromosome is evaluated and sorted. The algorithm then proceeds to select pairs for mating, perform crossover operations, and introduce mutation to maintain diversity. The process iterates by evaluating the fitness of the new population until the stopping criteria are met. Finally, the algorithm displays the final optimized solution. Through this iterative approach, the Genetic Algorithm explores the solution space, leveraging genetic operators to evolve and improve solutions over time, leading to an optimal or near-optimal solution for the given optimization problem.

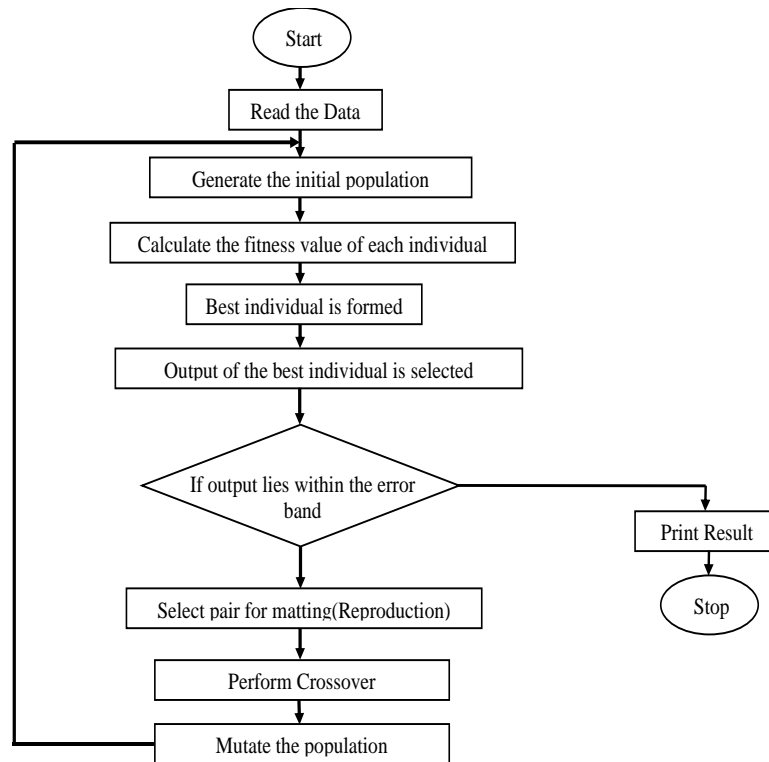


Figure 3.5 Flowchart of GA[21]

3.5 Modeling of EV charger and Analysis of EV charger

This section introduces two EV charger models employed in the study: a slow charger equipped with a 7.4 kW level-2 charger, and a fast charger featuring a 50 kW DC fast charger. Detailed implementation of these models was carried out using MATLAB/Simulink to analyze the responses of standard EV chargers when subjected to minor voltage disturbances. The simulated responses were then utilized to generate data for curve fitting methodologies applied to both static and dynamic load models.

The slow charger model, referred to as Approach A, utilized a diode rectifier and a DC/DC converter. On the other hand, Approach B, representing the fast charger model, employed a three-phase full bridge converter alongside a DC/DC converter. This two-stage power conversion, comprising AC/DC and DC/DC stages, offered inherent low-frequency ripple rejection and has been widely adopted in modern battery charger topologies. Additionally, power factor correction (PFC) control was implemented to maintain the power factor close to unity.

Approach A, with its simplified control structures, gained popularity in earlier EV charging stations, particularly in small residential chargers. However, it had certain functional limitations that rendered it unsuitable for smart charging applications.

Approach B utilizes a specific topology for EV fast charging, which includes a full bridge three-phase inverter and a DC/DC converter. This differs from the structure of approach A. In approach B, the control system requires a full bridge converter, which is a fully controllable AC/DC converter. It consists of both outer voltage and inner current control loops. The inner current control loop drives the converter based on dq currents, which are generated by the associated references of the outer control loops.

In most EV chargers, except for Tesla superchargers, there are DC/DC converters that regulate the charging DC voltage and control the power flow. This voltage regulation can be achieved using constant Pulse-Width Modulation (PWM) or by incorporating feedback control. Figure 3.6 depicts a block diagram illustrating the configuration of Approach B charger, while the corresponding simulation model is presented in Figure B.1.

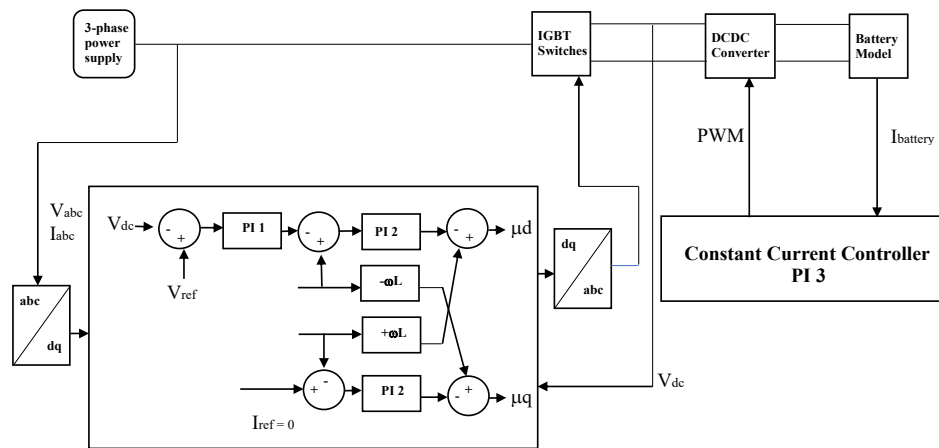


Figure 3.6 Block diagram of EV charger [1]

CHAPTER FOUR: RESULT AND DISCUSSION

4.1 Basic Introduction

This chapter presents the findings and discussions of a study conducted on the IEEE 33 bus radial distribution system. The study utilizes the ETAP software to develop a system model and perform load flow analysis. The simulation results are then compared with data provided by the IEEE Distribution System Analysis Subcommittee to validate their accuracy.

Based on the load flow analysis outcomes, protective elements are incorporated into the system. To determine the maximum, short-circuit current that can flow through the bus of the system, a short-circuit analysis is conducted. This analysis serves as a basis for optimizing the coordination between the protective elements.

The coordination optimization is accomplished using the Genetic Algorithm (GA) implemented through MATLAB software. The study also investigates the impact of integrating electric vehicle charging stations into the coordinated protection system. It reveals instances of mal-operation of the protective elements resulting from this integration, which are evaluated and discussed.

4.2 Simulation of IEEE 33 Bus Distribution system

IEEE-33 Bus Radial distribution system, is modeled and simulated in ETAP software. The normal current of buses 1-5 and paths are shown in Table 4.1. The normal current of all remaining buses are shown in Table B.1.

Table 4.1 Load Flow Report

LOAD FLOW REPORT					
From Bus	To Bus	MW	Mvar	Amp	%PF
Bus 1	Bus 2	3.927	2.459	211.3	84.8
Bus 2	Bus 1	-3.915	-2.452	211.3	84.7
	Bus 3	3.453	2.231	188.1	84.0
	Bus 19	0.361	0.161	18.1	91.3
Bus 3	Bus 2	-3.401	-2.205	188.1	83.9
	Bus 4	2.371	1.707	135.6	81.2

	Bus 23	0.940	0.457	48.5	89.9
Bus 4	Bus 3	-2.351	-1.697	135.6	81.1
	Bus 5	2.231	1.617	128.8	81.0
Bus 5	Bus 4	-2.212	-1.607	128.8	80.9

4.3 Protective device coordination

The study involves analyzing the Time-Current Characteristics (TCC) curve of various protective devices using the Star View toolbar in the ETAP software. This analysis helps to determine the fault clearing time difference between primary and backup protection devices at specific fault currents. As the number of branches increases, the problem of coordinating protective devices becomes more complex. To address this issue, the study uses Genetic Algorithm, which helps to solve the complex coordination problem and minimize the operating time of protective devices. By using this approach, the study aims to optimize the coordination between protective devices in a more efficient manner.

Figure 4.1 illustrates a graphical representation depicting the histogram of scores at each generation. It also showcases the vector entries of the individual with the highest fitness function value for each generation. Additionally, it presents the minimum, maximum, and average score values for each generation during the optimization process of protection coordination in the IEEE 33 bus distribution system, excluding Electric Vehicles (EVs).

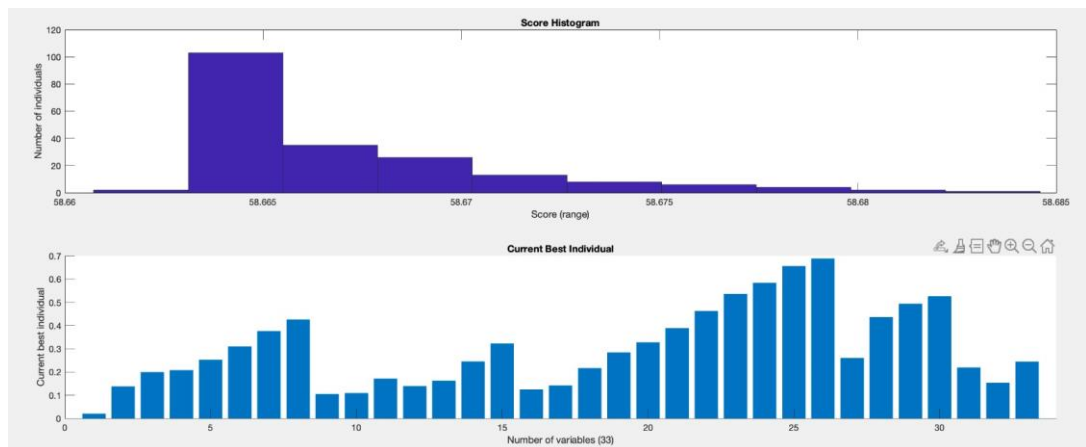


Figure 4.1 GA scores and histograms

The result of the optimum time multiplier setting achieved for each relay as a result of genetic algorithm by setting the required plug setting (PS) are shown in Table 4.2.

Table 4. 2 Plug Setting and Time Multiplier Setting

Relay No.	Plug Setting (PS)	Time Setting Multiplier (TSM)
1	1.900	0.244
2	1.896	0.153
3	2.643	0.219
4	5.200	0.526
5	5.267	0.494
6	4.887	0.436
7	4.673	0.260
8	18.743	0.688
9	21.770	0.656
10	21.333	0.584
11	23.704	0.536
12	23.289	0.463
13	22.400	0.389
14	24.114	0.328
15	33.067	0.284
16	39.200	0.217
17	45.422	0.141
18	65.733	0.124
19	52.578	0.323
20	62.333	0.245
21	78.933	0.162
22	106.133	0.139
23	18.524	0.172
24	19.200	0.108
25	34.743	0.105
26	12.507	0.425
27	12.996	0.375
28	12.015	0.309
29	11.686	0.251
30	13.138	0.207
31	28.952	0.199

32	40.373	0.137
33	2.013	0.020

4.4 FFT Analysis

The model of EV developed using MATLAB/Simulink is shown in the Figure B.1. The graph of current harmonics is analyzed to know the harmonics present in it and it is used later in the ETAP software to feed the EV source with same harmonics. The result of the voltage and current with harmonic component's graph is shown in the figure 4.2.

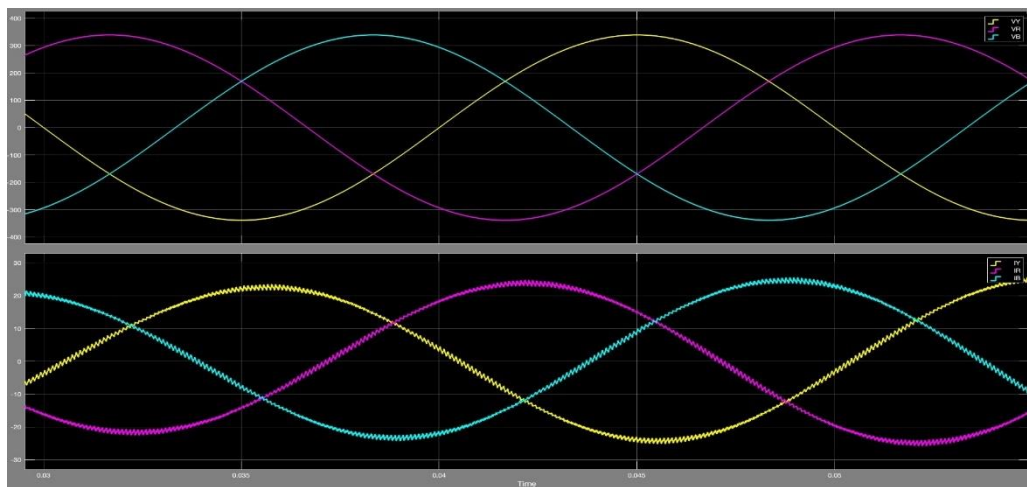


Figure 4.2 Voltage and current graph

FFT analysis stands for Fast Fourier Transform analysis, which is a mathematical technique used to convert a time-domain signal into its frequency-domain representation. The Fourier Transform is a mathematical function that decomposes a signal into its constituent frequencies. In other words, it allows us to see the individual frequency components that make up a complex signal. FFT is a faster algorithm used to implement the Fourier Transform. The FFT analysis of current is done in MATLAB and its FFT window and plot is shown in Figure 4.3 below.

To perform Fourier Transform (FT) analysis of an EV charger current signal in MATLAB, follow these steps:

1. Load the current signal data into MATLAB.
2. Use the "FFT" function in MATLAB to compute the FFT of the signal.
3. Use the "abs" function in MATLAB to compute the magnitude of the FFT signal.
4. Use the "angle" function in MATLAB to compute the phase of the FFT signal.

5. Create a frequency vector that corresponds to the FFT signal using the "linspace" function in MATLAB.
6. Plot the magnitude and phase of the FFT signal versus the frequency vector using the "plot" function in MATLAB.

The Harmonics order so obtained from FFT analysis with percentage of fundamental current and angles are shown in Table 4.3. The FFT analysis is shown in Figure 4.3.

Table 4. 3 Harmonics order present in EV charger

Harmonic Order	Percentage	Angle(degree)
0	25.45	90
1	100	156.6
2	19.99	269.4
3	15.44	244.8
4	5.68	213.2
5	2.58	214.3
6	2.27	219.5
7	1.83	212.2
8	1.64	212.1
9	1.37	208.5
10	1.11	207.3
11	1.01	202.4
12	0.92	197.2
13	0.88	221.4
14	0.84	208.8
15	0.73	205.2
16	0.87	203.9
17	0.62	202.3
18	0.62	186.5
19	0.65	189.3

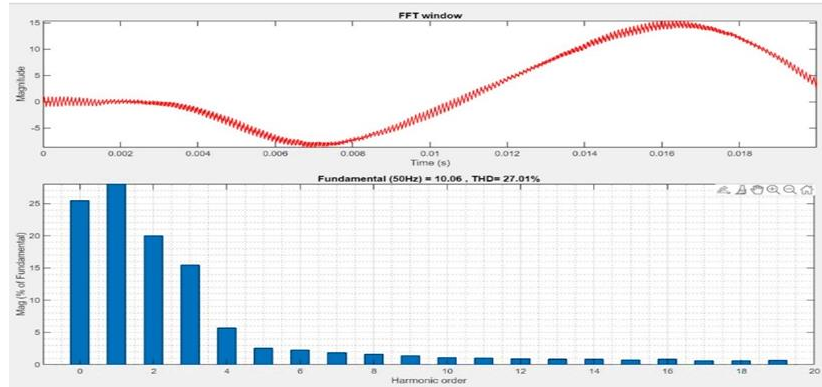


Figure 4.3 FFT analysis of current of EV charger

4.4.1 When lump loads are replaced with same ratings EV Charger load

In the standard 33 bus system, relays, circuit breakers (CB), and electric vehicle (EV) charging station loads with equivalent ratings to the existing lumped loads were installed. The value of current at different cases is presented in figure 4.4 and Table 4.4.

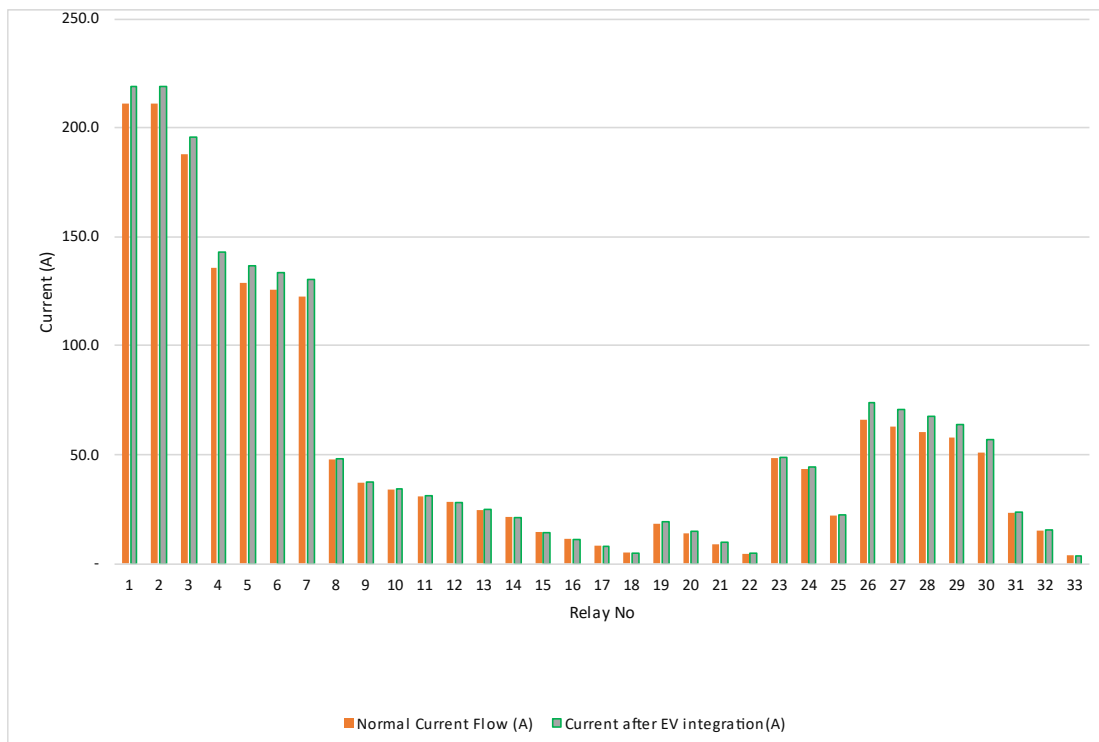


Figure 4.4 Current plot when loads are replaced with same ratings EV charger

Table 4.4 Difference of currents when loads are replaced with same ratings EV charger

Relay No.	Normal Current Flow (A)	Current after EV integration(A)	Difference
1	211.3	219.06	7.76
2	211.3	219.06	7.76
3	188.1	195.78	7.68
4	135.6	143.04	7.44
5	128.8	136.52	7.72
6	125.7	133.41	7.71
7	122.8	130.41	7.61
8	47.9	48.19	0.29
9	37.0	37.2	0.20
10	33.9	34.09	0.19
11	30.8	30.97	0.17
12	28.2	28.3	0.10
13	24.8	24.86	0.06
14	21.3	21.4	0.10
15	14.3	14.34	0.04
16	11.3	11.33	0.03
17	8.1	8.15	0.05
18	5.0	4.97	0.00
19	18.1	19.53	1.43
20	13.6	14.66	1.06
21	9.1	9.78	0.68
22	4.5	4.89	0.39
23	48.5	48.98	0.48
24	43.7	44.14	0.44
25	21.9	22.11	0.21
26	66.0	73.83	7.83
27	63.1	70.9	7.80
28	60.3	67.51	7.21
29	57.6	64.08	6.48
30	51.1	56.65	5.55
31	23.6	23.51	0.00
32	15.3	15.48	0.18
33	3.6	3.67	0.07

4.4.2 When lump loads are replaced with rating of Standard EV Charger load

The introduction of standard EV loads in some buses of the IEEE 33 bus system has led to the overloading of certain branches and subsequent tripping of relays. This is because the protective device's PSM value has been changed, surpassing the set value during normal operation. This means that the relay may trip even in the absence of an actual fault, disrupting the system's normal operation.

To ensure the proper functioning of the system, it is imperative to recheck and recalculate the relay settings for each affected relay. This will involve adjusting the protective device's settings to ensure that they are appropriate for the newly introduced EV loads, without compromising the system's overall safety and stability. Properly calibrated relay settings will prevent tripping during normal operation while still providing the necessary protection in the event of a fault. The values of current and the differences are tabulated in Table 4.5 and it is presented in figure 4.5.

Table 4.5 Difference of Currents when loads are replaced with Standard EV charger

Relay No.	Normal Current Flow (A)	Current after EV integration(A)	Trip Time T2(s)	Difference
2	211.3	265.08	10.77	53.78
3	188.1	235.60	13.33	47.50
4	135.6	182.61	18.68	47.01
5	128.8	175.89	21.67	47.09
6	125.7	172.73	21.61	47.03
7	122.8	169.71	14.74	46.91
8	47.9	49.11	normal operation	1.21
9	37.0	37.95	normal operation	0.95
10	33.9	34.79	normal operation	0.89
11	30.8	31.61	normal operation	0.81
12	28.2	28.90	normal operation	0.70
13	24.8	25.39	normal operation	0.59
14	21.3	21.86	normal operation	0.56
15	14.3	14.65	normal operation	0.35
16	11.3	11.57	normal operation	0.27
17	8.1	8.33	normal operation	0.23

18	5.0	5.08	normal operation	0.08
19	18.1	25.90	16.02	7.80
20	13.6	19.45	6.59	5.85
21	9.1	12.97	7.97	3.87
22	4.5	6.49	normal operation	1.99
23	48.5	48.92	normal operation	0.42
24	43.7	44.09	normal operation	0.39
25	21.9	22.08	normal operation	0.18
26	66.0	110.87	7.58	44.87
27	63.1	107.77	6.32	44.67
28	60.3	101.08	5.34	40.78
29	57.6	94.28	4.48	36.68
30	51.1	87.59	3.26	36.49
31	23.6	57.55	1.76	33.95
32	15.3	16.04	normal operation	0.74
33	3.6	3.80	normal operation	0.20

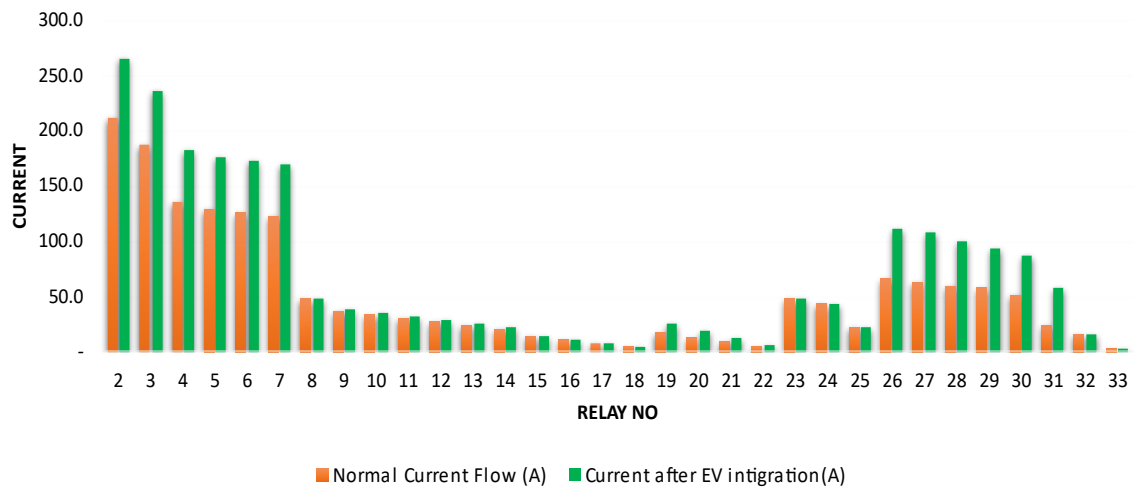


Figure 4.5 Current plot when loads are replaced with Standard EV charger loads

A fault has been created at bus 31 for both IEEE standard 33 bus model and EV equivalent load systems IEEE 33 Bus model. The tripping time of each relay and circuit breaker has been observed, and it appears that there is no change in the sequence of operation. However, there is a slight difference in the time of operation between the two systems.

The Table 4.6 and Table 4.7 below likely shows the different tripping times for the relays and circuit breakers in both systems, which can be used to compare their performance and reliability:

Table 4.6 Sequence of Operation of relay

<u>Sequence-of-Operation Event Summary Report</u>					
Symmetrical 3-Phase Fault at Bus31.					
Time (ms)	ID	If (kA)	T1 (ms)	T2 (ms)	Condition
900	Relay31	0.765	900		Phase - OC1 - 51 - Forward
980	CB31		80.0		Tripped by Relay31 Phase - OC1 - 51 - Forward
1158	Relay30	0.646	1158		Phase - OC1 - 51 - Forward
1238	CB30		80.0		Tripped by Relay30 Phase - OC1 - 51 - Forward
1508	Relay29	0.621	1508		Phase - OC1 - 51 - Forward
1588	CB29		80.0		Tripped by Relay29 Phase - OC1 - 51 - Forward
1915	Relay28	0.611	1915		Phase - OC1 - 51 - Forward
	CB28		80.0		1995
2408	Relay27	0.602	2408		Phase - OC1 - 51 - Forward
2488	CB27		80.0		Tripped by Relay27 Phase - OC1 - 51 - Forward
2820	Relay26	0.591	2820		Phase - OC1 - 51 - Forward
2900	CB26		80.0		Tripped by Relay26 Phase - OC1 - 51 - Forward
5470	Relay7	0.432	5470		Phase - OC1 - 51 - Forward
5550	CB7		80.0		Tripped by Relay7 Phase - OC1 - 51 - Forward
5824	Relay6	0.424	5824		Phase - OC1 - 51 - Forward
5904	CB6		80.0		Tripped by Relay6 Phase - OC1 - 51 - Forward
6706	Relay5	0.416	6706		Phase - OC1 - 51 - Forward
6786	CB5		80.0		Tripped by Relay5 Phase - OC1 - 51 - Forward
7495	Relay4	0.396	7495		Phase - OC1 - 51 - Forward
7575	CB4		80.0		Tripped by Relay4 Phase - OC1 - 51 - Forward
16994	Relay3	0.275	16994		Phase - OC1 - 51 - Forward
17074	CB3		80.0		Tripped by Relay3 Phase - OC1 - 51 - Forward

Table 4.7 Sequence of Operation of relay with EV load

<u>Sequence-of-Operation Event Summary Report</u>					
Symmetrical 3-Phase Fault at Bus31.					
Time (ms)	ID	If (kA)	T1 (ms)	T2 (ms)	Condition
900	Relay31	0.601	900		Phase - OC1 - 51 - Forward
980	CB31		80.0		Tripped by Relay31 Phase - OC1 - 51 - Forward
1194	Relay30	0.601	1194		Phase - OC1 - 51 - Forward
1274	CB30		80.0		Tripped by Relay30 Phase - OC1 - 51 - Forward
1531	Relay29	0.601	1531		Phase - OC1 - 51 - Forward
1611	CB29		80.0		Tripped by Relay29 Phase - OC1 - 51 - Forward
1929	Relay28	0.601	1929		Phase - OC1 - 51 - Forward
2009	CB28		80.0		Tripped by Relay28 Phase - OC1 - 51 - Forward
2409	Relay27	0.601	2409		Phase - OC1 - 51 - Forward
2489	CB27		80.0		Tripped by Relay27 Phase - OC1 - 51 - Forward
2823	Relay26	0.590	2823		Phase - OC1 - 51 - Forward
2903	CB26		80.0		Tripped by Relay26 Phase - OC1 - 51 - Forward
5606	Relay7	0.421	5606		Phase - OC1 - 51 - Forward
5686	CB7		80.0		Tripped by Relay7 Phase - OC1 - 51 - Forward
5982	Relay6	0.412	5982		Phase - OC1 - 51 - Forward
6062	CB6		80.0		Tripped by Relay6 Phase - OC1 - 51 - Forward

The single line diagram modelled in ETAP with equivalent EV load. The sequence of operation when fault is created at Bus 31 is shown in figure 4.8. The sequence of operation of relays are, relay 31 operates first as primary then relay 30, relay 29, relay 28, operate one after another as back up relay respectively.

One-Line Diagram - OLV1 (Star - Protection & Coordination)

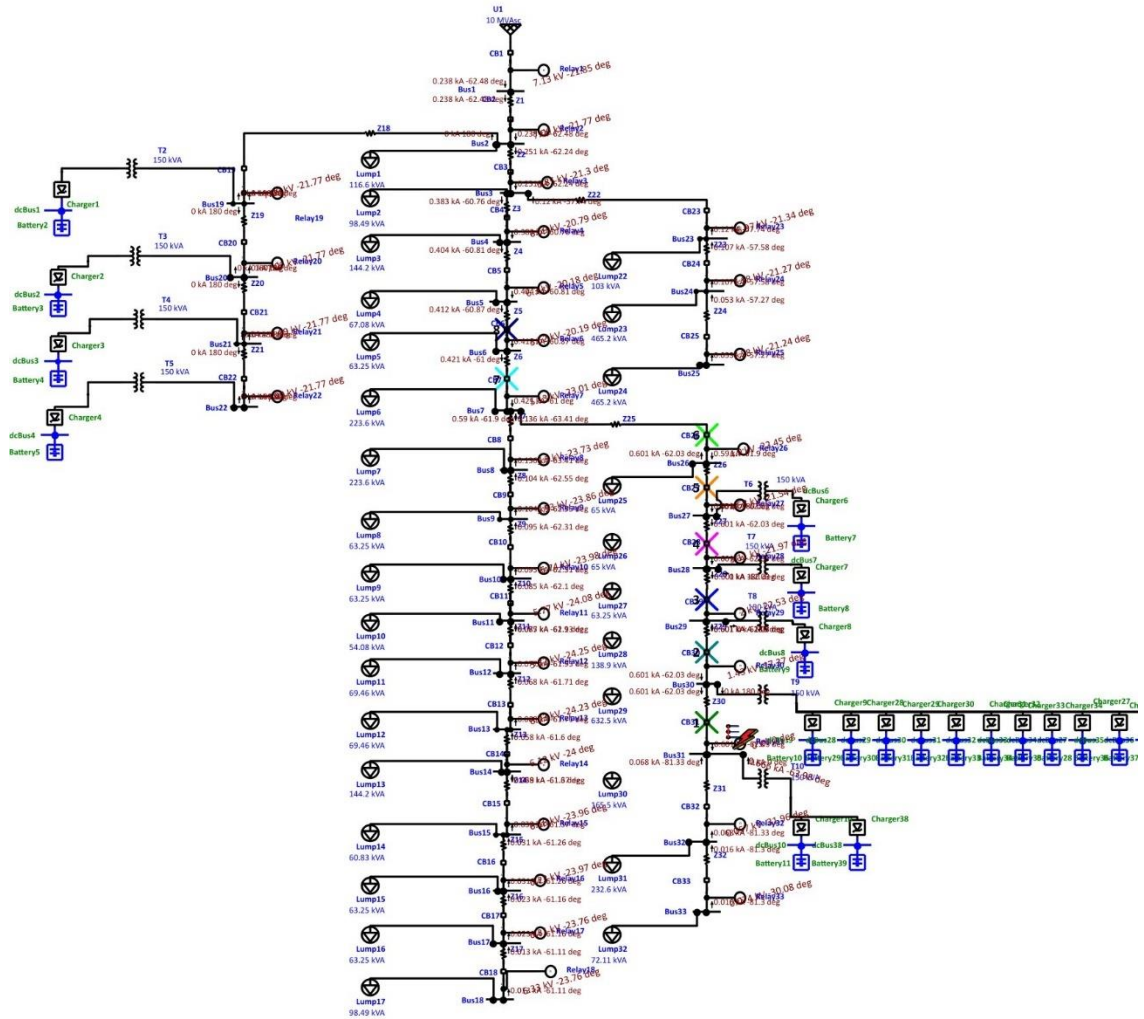


Figure 4.6 IEE 33 Bus with EV charging stations and Sequence trip

CHAPTER FIVE:

CONCLUSION AND RECOMMENDATION

In this study, the impact of integrating electric vehicle (EV) charging loads into the IEEE 33 bus distribution system was investigated, with a focus on relay and protection coordination. The replacement of standard loads with EV charging loads of the same rating introduced harmonic currents and total harmonic distortion (THD) into the system, resulting in a slight increase in the net RMS value of current. However, the tripping sequence of the relays remained unaltered, as indicated by the results presented in Table 4.4. No trip signal was generated since the current values were lower than the pickup current for each relay. In the event of a fault, the time of operation of relays is also changed, as seen in Table 4.6.

Nevertheless, when considering the scenario of bulk penetration of EV chargers into the network, the combined effect of increased load current and harmonic current led to overloading at the distribution buses. This resulted in relay trips, as shown in Table 4.5. In this case, the relay currents exceeded their rated values, causing the overloaded relays to trip. Notably, the tripping sequence remained unaltered, while the time of trip for each relay changed.

These findings highlight the significance of considering the harmonic currents and adjusting relay settings when integrating EV chargers into distribution systems. Future research should focus on further optimizing protection coordination techniques to accommodate the growing penetration of EVs, ensuring the stability and reliability of power grids amidst increasing environmental and energy demands. To ensure the proper protection of the system when integrating EV chargers, it is recommended to increase the pickup current for the relays. By adjusting the pickup current level, the relays will trip at higher current levels, effectively mitigating false tripping caused by harmonic currents introduced by EV chargers. Proper design and planning are essential in maintaining the reliability and protection of power distribution systems, particularly in scenarios with large-scale EV penetration

This study provides insights into the impact of EV integration on relay and protection coordination in the IEEE 33 bus distribution system. The results emphasize the need for

careful consideration of harmonic currents, along with adjusting pickup current levels, to ensure the reliable and protected operation of power distribution systems when integrating EV chargers.

REFERENCES

- [1] J. S. Farkhani, M. Zareein, H. Soroushmehr and H. M. SIEEE, "Coordination of Directional Overcurrent Protection Relay for Distribution Network With Embedded DG," 2019 5th Conference on Knowledge Based Engineering and Innovation (KBEI), Tehran, Iran, 2019, pp. 281-286, doi: 10.1109/KBEI.2019.8735025.
- [2] M. Sarkar, J. Jia, and G. Yang, "Distance Relay Performance in Future Converter Dominated Power Systems."
- [3] K. Prakash, A. Lallu, F. R. Islam, and K. A. Mamun, "Review of Power System Distribution Network Architecture," in *Proceedings - Asia-Pacific World Congress on Computer Science and Engineering 2016 and Asia-Pacific World Congress on Engineering 2016, APWC on CSE/APWCE 2016*, Institute of Electrical and Electronics Engineers Inc., Jun. 2017, pp. 124–130. doi: 10.1109/APWC-on-CSE.2016.030.
- [4] Institute of Electrical and Electronics Engineers., IEEE Industry Applications Society. Industrial and Commercial Power Systems Department., IEEE Standards Board., and American National Standards Institute., *IEEE recommended practice for protection and coordination of industrial and commercial power systems*. Institute of Electrical and Electronics Engineers, 2001.
- [5] A. Dubey and S. Santoso, "Electric Vehicle Charging on Residential Distribution Systems: Impacts and Mitigations," *IEEE Access*, vol. 3. Institute of Electrical and Electronics Engineers Inc., pp. 1871–1893, 2015. doi: 10.1109/ACCESS.2015.2476996.
- [6] F. Sehar, M. Pipattanasomporn, and S. Rahman, "Demand management to mitigate impacts of plug-in electric vehicle fast charge in buildings with renewables," *Energy*, vol. 120, pp. 642–651, 2017, doi: 10.1016/j.energy.2016.11.118.
- [7] P. T. Staats, W. M. Grady, A. Arapostathis, and R. S. Thallam, "A Statistical Analysis of the Effect of Electric Vehicle Battery Charging on Distribution System Harmonic Voltages," 1998.
- [8] X. P. Z. S. M. I. R. Shi, "Dynamic Impacts of Fast-charging Stations for "

- [9] K. Clement-Nyns, E. Haesen, and J. Driesen, “The impact of Charging plug-in hybrid electric vehicles on a residential distribution grid,” *IEEE Transactions on Power Systems*, vol. 25, no. 1, pp. 371–380, Feb. 2010, doi: 10.1109/TPWRS.2009.2036481.
- [10] A. M. Foley, I. J. Winning, and B. P. Ó. Gallachóir, “State-of-the-art in electric vehicle charging infrastructure,” in *2010 IEEE Vehicle Power and Propulsion Conference, VPPC 2010*, 2010. doi: 10.1109/VPPC.2010.5729014.
- [11] J. C. Gómez and M. M. Morcos, “Impact of EV battery chargers on the power quality of distribution systems,” *IEEE Transactions on Power Delivery*, vol. 18, no. 3, pp. 975–981, Jul. 2003, doi: 10.1109/TPWRD.2003.813873.
- [12] S. Deb, K. Tammi, K. Kalita, and P. Mahanta, “Impact of electric vehicle charging station load on distribution network,” *Energies (Basel)*, vol. 11, no. 1, 2018, doi: 10.3390/en11010178.
- [13] X. Xiao *et al.*, “Component-Based Modelling of EV Battery Chargers.”
- [14] F. Musavi, M. Edington, W. Eberle, and W. G. Dunford, “Evaluation and efficiency comparison of front end AC-DC plug-in hybrid charger topologies,” *IEEE Trans Smart Grid*, vol. 3, no. 1, pp. 413–421, Mar. 2012, doi: 10.1109/TSG.2011.2166413.
- [15] J.-S. Kim, G.-Y. Choe, H.-M. Jung, B.-K. Lee, Y.-J. Cho, and K.-B. Han, “Design and Implementation of a High-Efficiency On-Board Battery Charger for Electric Vehicles with Frequency Control Strategy.”
- [16] H. Tin, A. Abu-Siada, and M. S. Masoum, “Impact of Harmonics on the Performance of Over-Current Relays.”
- [17] E.-E. E. Portal, “The Basics Of Overcurrent Protection | EEP,” EEP - Electrical Engineering Portal. <https://electrical-engineering-portal.com/download-center/books-and-guides/relays/overcurrent-protection-basics>
- [18] Wikipedia Contributors, “Circuit breaker,” Wikipedia, Mar. 19, 2019. https://en.wikipedia.org/wiki/Circuit_breaker
- [19] S. Bala, “Protection Coordination Optimization in Distribution Network with Distributed Generation,” Aug. 2020.
- [20] H. Tian, D. Tzelepis, and P. N. Papadopoulos, “Electric vehicle charger static and dynamic modelling for power system studies,” *Energies (Basel)*, vol. 14, no. 7, Apr. 2021, doi: 10.3390/en14071801.

- [21] A. K. Pandey and S. Kirmani, "Implementation of genetic algorithm to find the optimal timing of overcurrent relays," 2016 IEEE International Power Electronics and Motion Control Conference (PEMC), Varna, Bulgaria, 2016, pp. 400-405, doi: 10.1109/EPEPEMC.2016.7752031.

APPENDIX

Appendix A: IEEE 33 Bus Distribution System

Table A.1 IEEE 33 Bus Distribution System Standard Data

Branch Name	Path of Bus	Load Name	Length (km)	Real Load (Kw)	Reactive Load(Kvar)	Resistance (Ohm/km)	Reactance (Ohm/km)
Branch1	1-2	L2	1	100	60	0.0922	0.0470
Branch2	2-3	L3	1	90	40	0.493	0.251
Branch3	3-4	L4	1	120	80	0.366	0.186
Branch4	4-5	L5	1	60	30	0.3811	0.1941
Branch5	5-6	L6	1	60	20	0.819	0.707
Branch6	6-7	L7	1	200	100	0.1872	0.6188
Branch7	7-8	L8	1	200	100	1.7114	1.2351
Branch8	8-9	L9	1	60	20	1.03	0.74
Branch9	9-10	L10	1	60	20	1.044	0.740
Branch10	10-11	L11	1	45	30	0.1966	0.0650
Branch11	11-12	L12	1	60	35	0.3744	0.1238
Branch12	12-13	L13	1	60	35	1.468	1.156
Branch13	13-14	L14	1	120	80	0.5416	0.7129
Branch14	14-15	L15	1	60	10	0.591	0.526
Branch15	15-16	L16	1	60	20	0.7463	0.5450
Branch16	16-17	L17	1	60	20	1.289	1.721

Branch17	17-18	L18	1	90	40	0.732	0.574
Branch18	2-19	L19	1	90	40	0.164	0.157
Branch19	19-20	L20	1	90	40	1.5042	1.3554
Branch20	20-21	L21	1	90	40	0.4095	0.4784
Branch21	21-22	L22	1	90	40	0.7089	0.9373
Branch22	3-23	L23	1	90	50	0.4512	0.3083
Branch23	23-24	L24	1	420	200	0.898	0.709
Branch24	24-25	L25	1	420	200	0.896	0.701
Branch25	6-26	L26	1	60	25	0.203	0.103
Branch26	26-27	L27	1	60	25	0.2842	0.1440
Branch27	27-28	L28	1	60	20	1.059	0.934
Branch28	28-29	L29	1	120	70	0.8042	0.7006
Branch29	29-30	L30	1	200	600	0.5075	0.2585
Branch30	30-31	L31	1	150	70	0.9744	0.9630
Branch31	31-32	L32	1	210	100	0.3105	0.3619
Branch32	32-33	L33	1	60	40	0.341	0.530

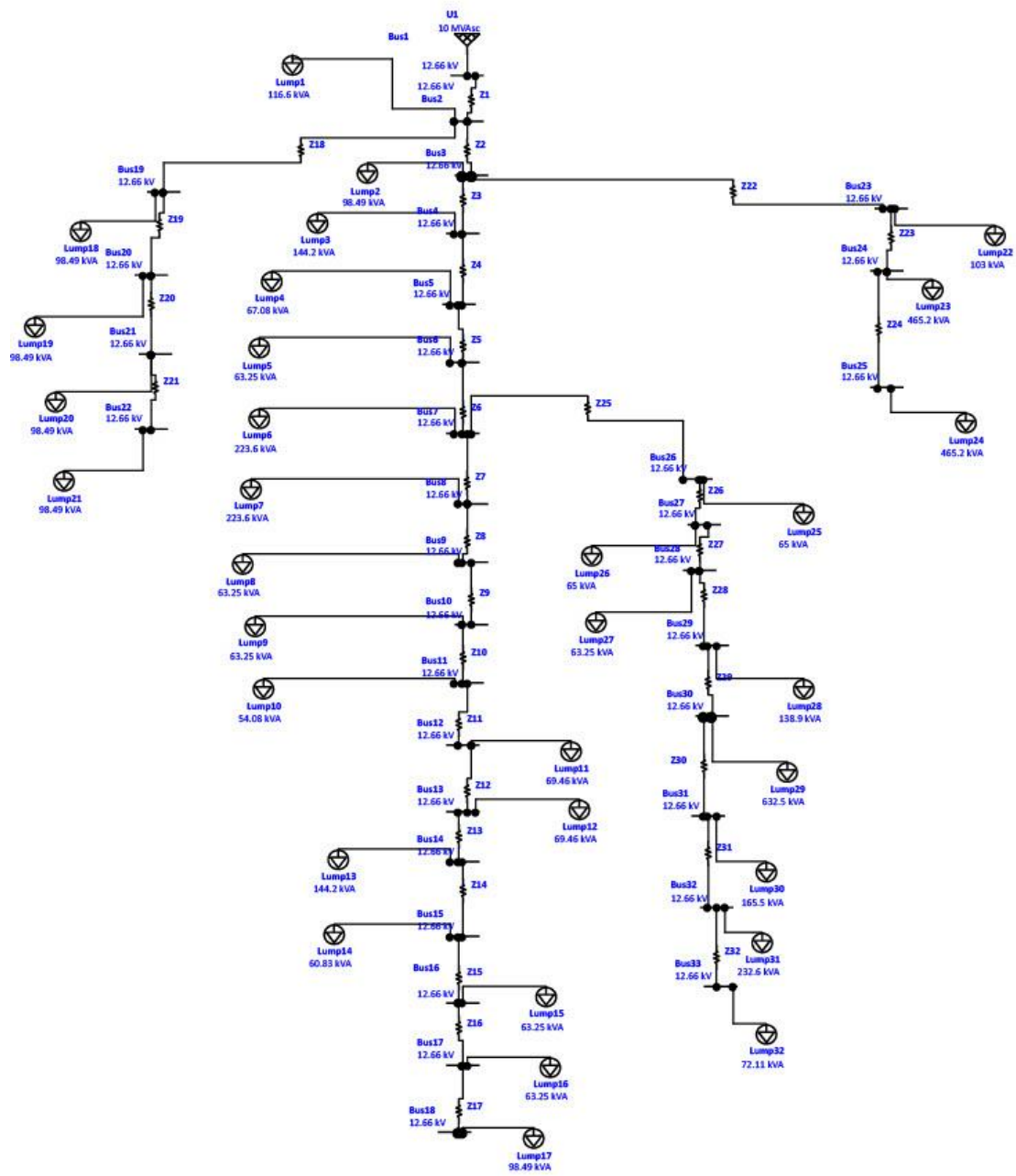


Figure A.1 ETAP model of 33 bus distribution network

Appendix B: Modelling and Results

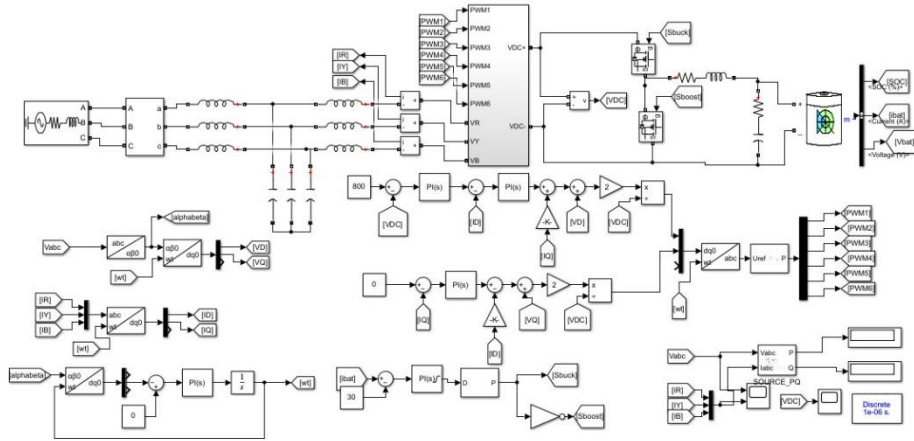


Figure B.1 EV charger model developed using MATLAB

Table B.1 Load flow report

Bus	Generation		Load		Voltage			Load Flow					
	ID	MW	Mvar	MW	Mvar	kV	% Mag.	Ang.	ID	MW	Mvar	Amp	% PF
Bus 1		3.927	2.459	0.000	0.000	12.660	100.000	0.0	Bus 2	3.927	2.459	211.3	84.8
Bus 2		0.000	0.000	0.100	0.060	12.660	99.702	0.0	Bus 1	-	-	211.3	84.7
									Bus 3	3.453	2.231	188.1	84.0
									Bus 19	0.361	0.161	18.1	91.3
Bus 3		0.000	0.000	0.090	0.040	12.660	98.286	0.1	Bus 2	-	-	188.1	83.9
									Bus 4	2.371	1.707	135.6	81.2
									Bus 23	0.940	0.457	48.5	89.9
Bus 4		0.000	0.000	0.120	0.080	12.660	97.533	0.2	Bus 3	-	-	135.6	81.1
									Bus 5	2.231	1.617	128.8	81.0
Bus 5		0.000	0.000	0.060	0.030	12.660	96.788	0.2	Bus 4	-	-	128.8	80.9
									Bus 6	2.152	1.577	125.7	80.7

Bus 6	0.000	0.000	0.060	0.020	12.660	94.933	0.1	Bus 5	-	-	125.7	80.8
								Bus 7	2.053	1.524	122.8	80.3
Bus 7	0.000	0.000	0.200	0.100	12.660	94.063	-0.2	Bus 6	-	-	122.8	80.7
								Bus 8	0.894	0.422	47.9	90.4
								Bus 26	0.951	0.974	66.0	69.9
Bus 8	0.000	0.000	0.200	0.100	12.660	93.576	-0.2	Bus 7	-	-	47.9	90.4
								Bus 9	0.689	0.320	37.0	90.7
Bus 9	0.000	0.000	0.060	0.020	12.660	92.945	-0.3	Bus 8	-	-	37.0	90.7
								Bus 10	0.624	0.297	33.9	90.3
Bus 10	0.000	0.000	0.060	0.020	12.660	92.360	-0.3	Bus 9	-	-	33.9	90.4
								Bus 11	0.561	0.274	30.8	89.8
Bus 11	0.000	0.000	0.045	0.030	12.660	92.273	-0.3	Bus 10	-	-	30.8	89.8
								Bus 12	0.515	0.244	28.2	90.4
Bus 12	0.000	0.000	0.060	0.035	12.660	92.122	-0.3	Bus 11	-	-	28.2	90.4
								Bus 13	0.454	0.209	24.8	90.9
Bus 13	0.000	0.000	0.060	0.035	12.660	91.507	-0.4	Bus 12	-	-	24.8	90.9
								Bus 14	0.392	0.172	21.3	91.6
Bus 14	0.000	0.000	0.120	0.080	12.660	91.279	-0.5	Bus 13	-	-	21.3	91.6
								Bus 15	0.271	0.091	14.3	94.8
Bus 15	0.000	0.000	0.060	0.010	12.660	91.137	-0.5	Bus 14	-	-	14.3	94.8
								Bus 16	0.211	0.081	11.3	93.4
Bus 16	0.000	0.000	0.060	0.020	12.660	90.999	-0.6	Bus 15	-	-	11.3	93.4
								Bus 17	0.150	0.060	8.1	92.8
Bus 17	0.000	0.000	0.060	0.020	12.660	90.795	-0.6	Bus 16	-	-	8.1	92.8
								Bus 18	0.090	0.040	5.0	91.4
Bus 18	0.000	0.000	0.090	0.040	12.660	90.734	-0.6	Bus 17	-	-	5.0	91.4
Bus 19	0.000	0.000	0.090	0.040	12.660	99.649	0.0	Bus 2	-	-	18.1	91.3
								Bus 20	0.271	0.121	13.6	91.3

Bus 20	0.000	0.000	0.090	0.040	12.660	99.291	-0.1	Bus 19	-	-	13.6	91.4
								Bus 21	0.180	0.080	9.1	91.4
Bus 21	0.000	0.000	0.090	0.040	12.660	99.221	-0.1	Bus 20	-	-	9.1	91.4
								Bus 22	0.090	0.040	4.5	91.4
Bus 22	0.000	0.000	0.090	0.040	12.660	99.157	-0.1	Bus 21	-	-	4.5	91.4
Bus 23	0.000	0.000	0.090	0.050	12.660	97.927	0.1	Bus 22	-	-	48.5	89.9
								Bus 24	0.846	0.405	43.7	90.2
Bus 24	0.000	0.000	0.420	0.200	12.660	97.260	0.0	Bus 23	-	-	43.7	90.3
								Bus 25	0.421	0.201	21.9	90.3
Bus 25	0.000	0.000	0.420	0.200	12.660	96.928	-0.1	Bus 24	-	-	21.9	90.3
Bus 26	0.000	0.000	0.060	0.025	12.660	93.868	-0.2	Bus 25	-	-	66.0	69.8
								Bus 27	0.889	0.948	63.1	68.4
Bus 27	0.000	0.000	0.060	0.025	12.660	93.609	-0.1	Bus 26	-	-	63.1	68.3
								Bus 28	0.825	0.921	60.3	66.7
Bus 28	0.000	0.000	0.060	0.020	12.660	92.454	-0.1	Bus 27	-	-	60.3	66.6
								Bus 29	0.754	0.891	57.6	64.6
Bus 29	0.000	0.000	0.120	0.070	12.660	91.623	0.0	Bus 28	-	-	57.6	64.5
								Bus 30	0.626	0.814	51.1	61.0
Bus 30	0.000	0.000	0.200	0.600	12.660	91.264	0.1	Bus 29	-	-	51.1	60.8
								Bus 31	0.422	0.212	23.6	89.4
Bus 31	0.000	0.000	0.150	0.070	12.660	90.844	0.0	Bus 30	-	-	23.6	89.4
								Bus 32	0.270	0.140	15.3	88.8
Bus 32	0.000	0.000	0.210	0.100	12.660	90.751	0.0	Bus 31	-	-	15.3	88.8
								Bus 33	0.060	0.040	3.6	83.2
Bus 33	0.000	0.000	0.060	0.040	12.660	90.723	0.0	Bus 32	-	-	3.6	83.2

Table B.2 Current distortions due to harmonics

System Harmonics Branch Information

Bus		Current Distortion											
From Bus ID	To Bus ID	Fund. Amp	RMS Amp	ASUM Amp	THD %	TIF	IT Amp	ITn Amp	ITn Amp	TIHD %	TSHD %	THDG %	THDS %
Bus1	Bus2	264.12	265.08	293.17	8.50	5.29	1401.62	1401.62	0.00	0.00	0.00	8.50	8.50
Bus2	Bus1	264.12	265.08	293.17	8.50	5.29	1401.62	1401.62	0.00	0.00	0.00	8.50	8.50
	Bus3	235.03	235.60	259.67	6.93	9.92	2336.42	2336.42	0.00	0.00	0.00	6.93	6.93
	Bus19	24.43	25.90	38.99	35.15	77.00	1994.05	1994.05	0.00	0.00	0.00	35.15	35.15
Bus3	Bus2	235.03	235.60	259.67	6.93	9.92	2336.42	2336.42	0.00	0.00	0.00	6.93	6.93
	Bus4	181.80	182.61	206.96	9.42	11.70	2136.47	2136.47	0.00	0.00	0.00	9.42	9.42
	Bus23	48.71	48.92	57.03	9.42	37.50	1834.79	1834.79	0.00	0.00	0.00	9.42	9.42
Bus4	Bus3	181.80	182.61	206.96	9.42	11.70	2136.47	2136.47	0.00	0.00	0.00	9.42	9.42
	Bus5	175.03	175.89	200.60	9.93	12.64	2223.81	2223.81	0.00	0.00	0.00	9.93	9.93
Bus5	Bus4	175.03	175.89	200.60	9.93	12.64	2223.81	2223.81	0.00	0.00	0.00	9.93	9.93
	Bus6	171.84	172.73	197.60	10.18	13.17	2275.52	2275.52	0.00	0.00	0.00	10.18	10.18
Bus6	Bus5	171.84	172.73	197.60	10.18	13.17	2275.52	2275.52	0.00	0.00	0.00	10.18	10.18
	Bus7	168.80	169.71	194.75	10.42	13.75	2332.95	2332.95	0.00	0.00	0.00	10.42	10.42
Bus7	Bus6	168.80	169.71	194.75	10.42	13.75	2332.95	2332.95	0.00	0.00	0.00	10.42	10.42
	Bus8	48.89	49.11	57.43	9.52	40.03	1965.95	1965.95	0.00	0.00	0.00	9.52	9.52
	Bus26	108.95	110.87	140.75	18.87	37.59	4167.63	4167.63	0.00	0.00	0.00	18.87	18.87
Bus8	Bus7	48.89	49.11	57.43	9.52	40.03	1965.95	1965.95	0.00	0.00	0.00	9.52	9.52
	Bus9	37.78	37.95	44.33	9.46	39.73	1507.80	1507.80	0.00	0.00	0.00	9.46	9.46
Bus9	Bus8	37.78	37.95	44.33	9.46	39.73	1507.80	1507.80	0.00	0.00	0.00	9.46	9.46
	Bus10	34.64	34.79	40.60	9.40	39.43	1371.83	1371.83	0.00	0.00	0.00	9.40	9.40
Bus10	Bus9	34.64	34.79	40.60	9.40	39.43	1371.83	1371.83	0.00	0.00	0.00	9.40	9.40
	Bus11	31.47	31.61	36.86	9.34	39.12	1236.69	1236.69	0.00	0.00	0.00	9.34	9.34
Bus11	Bus10	31.47	31.61	36.86	9.34	39.12	1236.69	1236.69	0.00	0.00	0.00	9.34	9.34
	Bus12	28.77	28.90	33.71	9.37	39.28	1135.21	1135.21	0.00	0.00	0.00	9.37	9.37
Bus12	Bus11	28.77	28.90	33.71	9.37	39.28	1135.21	1135.21	0.00	0.00	0.00	9.37	9.37
	Bus13	25.28	25.39	29.63	9.38	39.40	1000.29	1000.29	0.00	0.00	0.00	9.38	9.38
Bus13	Bus12	25.28	25.39	29.63	9.38	39.40	1000.29	1000.29	0.00	0.00	0.00	9.38	9.38
	Bus14	21.76	21.86	25.53	9.42	39.62	866.24	866.24	0.00	0.00	0.00	9.42	9.42
Bus14	Bus13	21.76	21.86	25.53	9.42	39.62	866.24	866.24	0.00	0.00	0.00	9.42	9.42
	Bus15	14.58	14.65	17.17	9.64	40.88	598.73	598.73	0.00	0.00	0.00	9.64	9.64
Bus15	Bus14	14.58	14.65	17.17	9.64	40.88	598.73	598.73	0.00	0.00	0.00	9.64	9.64
	Bus16	11.52	11.57	13.54	9.52	40.22	465.43	465.43	0.00	0.00	0.00	9.52	9.52
Bus16	Bus15	11.52	11.57	13.54	9.52	40.22	465.43	465.43	0.00	0.00	0.00	9.52	9.52
	Bus17	8.29	8.33	9.73	9.46	39.90	332.25	332.25	0.00	0.00	0.00	9.46	9.46
Bus17	Bus16	8.29	8.33	9.73	9.46	39.90	332.25	332.25	0.00	0.00	0.00	9.46	9.46
	Bus18	5.05	5.08	5.92	9.34	39.26	199.33	199.33	0.00	0.00	0.00	9.34	9.34
Bus18	Bus17	5.05	5.08	5.92	9.34	39.26	199.33	199.33	0.00	0.00	0.00	9.34	9.34
Bus19	Bus2	24.43	25.90	38.99	35.15	77.00	1994.05	1994.05	0.00	0.00	0.00	35.15	35.15
	Bus20	18.35	19.45	29.28	35.12	76.97	1497.14	1497.14	0.00	0.00	0.00	35.12	35.12
	Bus35	6.08	6.27	8.76	24.75	63.66	398.86	398.86	0.00	0.00	0.00	24.75	24.75

Table B.3 Current distortions due to harmonics

Bus		Current Distortion											
From Bus ID	To Bus ID	Fund. Amp	RMS Amp	ASUM Amp	THD %	TIF	IT Amp	ITb Amp	ITr Amp	THD %	TSHD %	THDG %	THDS %
Bus20	Bus19	18.35	19.45	29.28	35.12	76.97	1497.14	1497.14	0.00	0.00	0.00	35.12	35.12
	Bus21	12.24	12.97	19.53	35.12	76.96	998.38	998.38	0.00	0.00	0.00	35.12	35.12
	Bus36	6.11	6.30	8.80	24.72	63.64	400.62	400.62	0.00	0.00	0.00	24.72	24.72
Bus21	Bus20	12.24	12.97	19.53	35.12	76.96	998.38	998.38	0.00	0.00	0.00	35.12	35.12
	Bus22	6.12	6.49	9.77	35.11	76.95	499.32	499.32	0.00	0.00	0.00	35.11	35.11
	Bus37	6.12	6.30	8.81	24.72	63.63	400.95	400.95	0.00	0.00	0.00	24.72	24.72
Bus22	Bus21	6.12	6.49	9.77	35.11	76.95	499.32	499.32	0.00	0.00	0.00	35.11	35.11
	Bus38	6.12	6.31	8.82	24.72	63.63	401.26	401.26	0.00	0.00	0.00	24.72	24.72
Bus23	Bus3	48.71	48.92	57.03	9.42	37.50	1834.79	1834.79	0.00	0.00	0.00	9.42	9.42
	Bus24	43.90	44.09	51.41	9.43	37.55	1655.78	1655.78	0.00	0.00	0.00	9.43	9.43
Bus24	Bus23	43.90	44.09	51.41	9.43	37.55	1655.78	1655.78	0.00	0.00	0.00	9.43	9.43
	Bus25	21.99	22.08	25.74	9.39	37.42	826.48	826.48	0.00	0.00	0.00	9.39	9.39
Bus25	Bus24	21.99	22.08	25.74	9.39	37.42	826.48	826.48	0.00	0.00	0.00	9.39	9.39
Bus26	Bus7	108.95	110.87	140.75	18.87	37.59	4167.63	4167.63	0.00	0.00	0.00	18.87	18.87
	Bus27	105.75	107.77	137.94	19.62	39.75	4283.99	4283.99	0.00	0.00	0.00	19.62	19.62
Bus27	Bus26	105.75	107.77	137.94	19.62	39.75	4283.99	4283.99	0.00	0.00	0.00	19.62	19.62
	Bus28	99.34	101.08	129.05	18.79	39.06	3947.92	3947.92	0.00	0.00	0.00	18.79	18.79
	Bus40	6.66	6.86	9.55	24.36	63.35	434.30	434.30	0.00	0.00	0.00	24.36	24.36
Bus28	Bus27	99.34	101.08	129.05	18.79	39.06	3947.92	3947.92	0.00	0.00	0.00	18.79	18.79
	Bus29	92.81	94.28	120.13	17.89	38.50	3630.15	3630.15	0.00	0.00	0.00	17.89	17.89
	Bus41	6.81	7.01	9.75	24.28	63.31	443.85	443.85	0.00	0.00	0.00	24.28	24.28
Bus29	Bus28	92.81	94.28	120.13	17.89	38.50	3630.15	3630.15	0.00	0.00	0.00	17.89	17.89
	Bus30	86.21	87.59	110.55	18.01	41.21	3609.93	3609.93	0.00	0.00	0.00	18.01	18.01
	Bus42	6.92	7.12	10.63	23.66	113.33	806.43	806.43	0.00	0.00	0.00	23.66	23.66
Bus30	Bus29	86.21	87.59	110.55	18.01	41.21	3609.93	3609.93	0.00	0.00	0.00	18.01	18.01
	Bus31	30.64	30.75	35.70	8.71	34.85	1071.72	1071.72	0.00	0.00	0.00	8.71	8.71
	Bus44	56.19	57.55	77.92	22.12	60.56	3485.20	3485.20	0.00	0.00	0.00	22.12	22.12
Bus31	Bus30	30.64	30.75	35.70	8.71	34.85	1071.72	1071.72	0.00	0.00	0.00	8.71	8.71
	Bus32	15.96	16.04	19.07	10.36	50.26	806.16	806.16	0.00	0.00	0.00	10.36	10.36
	Bus45	14.78	15.15	20.69	22.57	62.58	948.04	948.04	0.00	0.00	0.00	22.57	22.57
Bus32	Bus31	15.96	16.04	19.07	10.36	50.26	806.16	806.16	0.00	0.00	0.00	10.36	10.36
	Bus33	3.78	3.80	4.48	9.88	47.12	179.18	179.18	0.00	0.00	0.00	9.88	9.88
Bus33	Bus32	3.78	3.80	4.48	9.88	47.12	179.18	179.18	0.00	0.00	0.00	9.88	9.88
Bus35	Bus19	185.54	199.22	337.69	39.10	79.89	15915.73	12167.71	10259.49	0.00	0.00	39.10	39.10
Bus36	Bus20	186.44	200.13	339.08	39.03	79.83	15977.21	12221.20	10291.44	0.00	0.00	39.03	39.03
Bus37	Bus21	186.61	200.31	339.34	39.01	79.82	15989.08	12231.50	10297.62	0.00	0.00	39.01	39.01
Bus38	Bus22	186.76	200.46	339.58	39.00	79.81	15999.69	12240.72	10303.14	0.00	0.00	39.00	39.00
Bus40	Bus27	203.20	217.30	365.13	37.89	79.05	17177.62	13248.80	10933.44	0.00	0.00	37.89	37.89
Bus41	Bus28	207.83	222.04	372.35	37.61	78.92	17523.96	13540.17	11124.43	0.00	0.00	37.61	37.61
Bus42	Bus29	211.24	221.05	394.63	30.84	168.47	37241.52	24600.83	27959.44	0.00	0.00	30.84	30.84
Bus44	Bus30	1714.11	1780.85	2772.46	28.18	72.25	128674.30	106319.50	72479.28	0.00	0.00	28.18	28.18
Bus45	Bus31	450.78	472.54	756.24	31.44	76.36	36083.17	28920.99	21577.11	0.00	0.00	31.44	31.44

Appendix C: Genetic Algorithm Source Code

```

%%%%%%%%%% Genetic Algorithm Function %%%%%%%%%%%
ObjectiveFunction = @RcordDhau; % RELAYCOORDINATION function
nvars = 33 ; % Number of variables
LB = zeros(1,nvars); % Lower bound
UB = 10*ones(1,nvars); % Upper bound
ConstraintFunction = @ConstDhau; % CONSTRAINT function
%rng(1,'twister') % for reproducibility
options=gaoptimset('Display','iter')
%[x,fval] = ga(ObjectiveFunction,nvars,...
    % [],[],[],[],LB,UB,ConstraintFunction,[],options)
options = optimoptions('ga','PlotFcn',{'gaplotscorediversity',
'gplotbestindiv','gplotrange'});
[x,fval]=ga(ObjectiveFunction,nvars,...
    [],[],[],[],LB,UB,ConstraintFunction,[],options)
%clc;
%clear;

%%%%%%%%%% CONSTRAINT Function %%%%%%%%%%%
function [c, ceq] = constraintrelay(x)
% Detailed explanation goes here
%%%%%%%%%% CONSTRAINT Function %%%%%%%%%%%
function [c, ceq] = constraintrelay(x)
% Detailed explanation goes here
c=[0.3-21.67*x(33)+32.62*x(32);          0.3-32.62*x(32)+3.40*x(15);          0.3-
32.62*x(32)+21.40*x(31);    0.3-3.40*x(15)+3.25*x(14);    0.3-3.25*x(14)+3.07*x(13);
0.3-3.07*x(13)+1.43*x(12);    0.3-21.40*x(31)+4.66*x(11);    0.3-4.66*x(11)+4.60*x(10);
0.3-4.60*x(10)+1.90*x(9);    0.3-21.40*x(31)+8.35*x(30);    0.3-8.35*x(30)+8.29*x(29);
0.3-8.29*x(29)+8.69*x(28);    0.3-8.69*x(28)+13.41*x(27);    0.3-13.41*x(27)+4.64*x(26);
0.3-.64*x(26)+4.41*x(25);    0.3-4.41*x(25)+4.44*x(24);    0.3-4.44*x(24)+4.28*x(23);
0.3-4.28*x(23)+4.31*x(22);    0.3-4.31*x(22)+4.36*x(21);    0.3-4.36*x(21)+4.26*x(20);

```

```

0.3-4.26*x(20)+3.86*x(19); 0.3-3.86*x(19)+3.68*x(18); 0.3-3.68*x(18)+3.53*x(17);
0.3-3.53*x(17)+1.60*x(16); 0.3-13.41*x(27)+5.40*x(8); 0.3-5.40*x(8)+5.32*x(7);
0.3-5.32*x(7)+5.49*x(6); 0.3-5.49*x(6)+5.56*x(5); 0.3-5.56*x(5)+5.30*x(4); 0.3-
5.30*x(4)+4.02*x(3); 0.3-4.02*x(3)+3.65*x(2); 0.3-3.65*x(2)+9.93*x(1); 0.2-
21.67*x(33); 0.2-32.62*x(32); 0.2-21.40*x(31); 0.2-8.35*x(30); 0.2-8.29*x(29); 0.2-
8.69*x(28); 0.2-13.41*x(27); 0.2-4.64*x(26); 0.2-4.41*x(25); 0.2-4.44*x(24); 0.2-
4.28*x(23); 0.2-4.31*x(22); 0.2-4.36*x(21); 0.2-4.26*x(20); 0.2-3.86*x(19); 0.2-
3.68*x(18); 0.2-3.53*x(17); 0.2-1.60*x(16); 0.2-3.40*x(15); 0.2-3.25*x(14); 0.2-
3.07*x(13); 0.2-1.43*x(12); 0.2-4.66*x(11); 0.2-4.60*x(10); 0.2-1.90*x(9); 0.2-
5.40*x(8); 0.2-5.32*x(7); 0.2-5.49*x(6); 0.2-5.56*x(5); 0.2-5.30*x(4); 0.2-
4.02*x(3); 0.2-3.65*x(2); 0.2-9.93*x(1);
]
ceq = [];
end

```

```

%%%%%%%%%%%%%%RELAYCOORDINATIONFUNCTION%%%%%%%%%%%%%%
function y = relaycoordination(x)
% Summary of this function goes here
% y is the main optimize solution to be obtained
y = 9.93*x(1)+3.65*x(2)+4.02*x(3)...
+5.30*x(4)+5.56*x(5)+5.49*x(6)+5.32*x(7)...
+5.40*x(8)+1.90*x(9)+4.60*x(10)...
+4.66*x(11)+1.43*x(12)+3.07*x(13)...
+3.25*x(14)+3.40*x(15)+1.60*x(16)...
+3.53*x(17)+3.68*x(18)+3.86*x(19)...
+4.26*x(20)+4.36*x(21)+4.31*x(22)...
+4.28*x(23)+4.44*x(24)+4.41*x(25)...
+4.64*x(26)+13.41*x(27)+8.69*x(28)...
+8.29*x(29)+8.35*x(30)+21.40*x(31)+32.62*x(32)+21.66*x(33);
end

```


ANALYSIS OF THE IMPACT OF EV PENETRATION ON PROTECTION COORDINATION

ORIGINALITY REPORT

19%

SIMILARITY INDEX

PRIMARY SOURCES

- | | | |
|---|--|-----------------|
| 1 | www.researchgate.net
Internet | 305 words — 2% |
| 2 | Anand K Pandey, Sheeraz Kirmani. "Implementation of genetic algorithm to find the optimal timing of overcurrent relays", 2016 IEEE International Power Electronics and Motion Control Conference (PEMC), 2016
Crossref | 233 words — 2% |
| 3 | strathprints.strath.ac.uk
Internet | 173 words — 1% |
| 4 | www.mdpi.com
Internet | 163 words — 1% |
| 5 | Salah Kamel, Ahmed Shaban, Ahmed Korashy, Loai Nasrat, Juan Yu, Shuocheng Wang. "Short Circuit Analysis and Coordination of Overcurrent Relays for a Realistic Substation Located in Upper Egypt", 2019 IEEE Innovative Smart Grid Technologies - Asia (ISGT Asia), 2019
Crossref | 128 words — 1% |
| 6 | openaccess.izu.edu.tr
Internet | 53 words — < 1% |
| 7 | Hitesh Agarwal, J.N. Rai. "Protection Coordination of Distributed System with Distributed | 51 words — < 1% |

Generation", 2022 International Conference on Intelligent
Controller and Computing for Smart Power (ICICCSP), 2022

Crossref

-
- 8 pdfcoffee.com 48 words — < 1%
Internet
-
- 9 www.yumpu.com 44 words — < 1%
Internet
-
- 10 B. Hussain, S. M. Sharkh, S. Hussain, M. A. Abusara. "An Adaptive Relaying Scheme for Fuse Saving in Distribution Networks With Distributed Generation", IEEE Transactions on Power Delivery, 2013 43 words — < 1%
Crossref
-
- 11 K. Prakash, A. Lallu, F.R. Islam, K.A. Mamun. "Review of Power System Distribution Network Architecture", 2016 3rd Asia-Pacific World Congress on Computer Science and Engineering (APWC on CSE), 2016 43 words — < 1%
Crossref
-
- 12 www.coursehero.com 41 words — < 1%
Internet
-
- 13 torquecontrol.eaton.com 36 words — < 1%
Internet
-
- 14 zero.sci-hub.se 34 words — < 1%
Internet
-
- 15 Vasiliki Vita. "Development of a Decision-Making Algorithm for the Optimum Size and Placement of Distributed Generation Units in Distribution Networks", Energies, 2017 32 words — < 1%
Crossref

- 16 Internet 32 words — < 1%
-
- 17 Ch.V.S.S. Sailaja, P.V.N. Prasad. "Determination of optimal distributed generation size for losses, protection Co-ordination and reliability Evaluation Using ETAP", 2016 Biennial International Conference on Power and Energy Systems: Towards Sustainable Energy (PESTSE), 2016
Crossref 29 words — < 1%
-
- 18 Shubhangi B. Walke, Nayana N. Jangle. "Review: Methods for relay coordination", 2017 International Conference on Computing Methodologies and Communication (ICCMC), 2017
Crossref 28 words — < 1%
-
- 19 ebin.pub Internet 27 words — < 1%
-
- 20 Odiyur V.G. Swathika, Udayanga Hemapala. "Optimized Overcurrent Relay Coordination in a Microgrid System", Recent Advances in Computer Science and Communications, 2021
Crossref 24 words — < 1%
-
- 21 Dingyü Xue. "Solving Optimization Problems with MATLAB®", Walter de Gruyter GmbH, 2020
Crossref 23 words — < 1%
-
- 22 in.mathworks.com Internet 23 words — < 1%
-
- 23 slidetodoc.com Internet 21 words — < 1%
-
- 24 en.wikipedia.org Internet 20 words — < 1%